Subduction-modified oceanic crust mixed with a depleted mantle reservoir in the sources of the Karoo continental flood basalt province

Jussi S. Heinonen [a,b] (corresponding author, jussi.s.heinonen@helsinki.fi, +35850-3185304)

Richard W. Carlson [b] (carlson@dtm.ciw.edu)

Teal R. Riley [c] (trr@bas.ac.uk)

Arto V. Luttinen [a] (arto.luttinen@helsinki.fi)

Mary F. Horan [b] (horan@dtm.ciw.edu)

[a] Finnish Museum of Natural History, P.O. Box 44, 00014 University of Helsinki, Finland

[b] Department of Terrestrial Magnetism, Carnegie Institution of Washington, 5241 Broad Branch Road, NW Washington, D.C. 20015, USA

[c] British Antarctic Survey, Madingley Road, High Cross, Cambridge, Cambridgeshire CB3 0ET, United Kingdom

Abstract

The great majority of continental flood basalts (CFBs) have a marked lithospheric geochemical signature, suggesting derivation from the continental lithosphere, or contamination by it. Here we present new Pb and Os isotopic data and review previously published major element, trace element, mineral chemical, and Sr and Nd isotopic data for geochemically unusual mafic and ultramafic dikes located in the Antarctic segment (Ahlmannryggen, western Dronning Maud Land) of the Karoo CFB province. Some of the dikes show evidence of minor contamination with continental crust, but the least contaminated dikes exhibit depleted mantle –like initial ε_{Nd} (+9) and $^{187}Os/^{188}Os$ (0.1244–0.1251) at 180 Ma. In contrast, their initial Sr and Pb isotopic compositions ($^{87}Sr/^{86}Sr$ = 0.7035–0.7062, $^{206}Pb/^{204}Pb$ = 18.2–18.4, $^{207}Pb/^{204}Pb$ = 15.49–15.52, $^{208}Pb/^{204}Pb$ = 37.7–37.9 at 180 Ma) are more enriched than expected for depleted mantle, and the major element and mineral chemical evidence indicate contribution from (recycled) pyroxenite sources. Our Sr, Nd, Pb, and Os isotopic and trace element modeling indicate mixed peridotite-pyroxenite sources that contain ~10–30 % of seawater-altered and subduction-modified MORB with a recycling age of less than 1.0 Ga entrained in a depleted Os-rich peridotite matrix. Such a source would explain the unusual combination of elevated initial $^{87}Sr/^{86}Sr$ and Pb isotopic ratios and relative depletion in LILE, U, Th, Pb and LREE, high initial ε_{Nd}, and low initial $^{187}Os/^{188}Os$.

Although the sources of the dikes probably did not play a major part in the generation of the Karoo CFBs in general, different kind of recycled source components (e.g., sediment-influenced) would be more difficult to distinguish from lithospheric CFB geochemical signatures. In addition to underlying continental lithosphere, the involvement of recycled sources in causing the apparent lithospheric geochemical affinity of CFBs should thus be carefully assessed in every case.

Keywords: Large igneous province; Continental flood basalt; Karoo; Picrite; Mantle source; Crustal recycling

1. Introduction

Continental flood basalts (CFBs) represent the most voluminous magmatic activity on the continents. They are commonly associated with the early stages of continental breakup, but whether they arise due to processes related to the continental lithosphere (e.g., thinning, delamination, and insulation) or instead derive from melting of a deep mantle plume, remains an issue of discussion (e.g., Anderson, 2005; Beccaluva et al., 2009; Campbell, 2005; Coltice et al., 2009; Elkins-Tanton and Hager, 2000; Jourdan et al., 2007; Sobolev et al., 2011b). CFBs generally show highly variable trace element and isotopic compositions, often attributed to assimilation with, or derivation from, continental lithosphere (e.g., Carlson et al., 1981; Hawkesworth et al., 1992; Jourdan et al., 2007, Lightfoot et al., 1990; Luttinen and Furnes, 2000; Molzahn et al., 1996; Pik et al., 1999; Sano et al., 2001).

The role of sublithospheric mantle sources in CFB petrogenesis remains poorly constrained. On some occasions, Mg-rich melts derived from the convecting mantle have risen within thick continents so rapidly or through such cold or infertile material that they have preserved their primary geochemical signatures. Lavas and dikes crystallized from such melts have been recognized on the basis of anomalous compositional characteristics (e.g., high initial ε_{Nd}) that are not compatible with continental lithospheric sources. Instead, depleted MORB mantle (DMM), recycled oceanic lithosphere, and hotspot-related geochemical reservoirs such as non-chondritic primitive mantle have been suggested to be possible source components (e.g., Carlson et al., 2006; Day et al., 2013; Fram and Lesher, 1997; Heinonen et al., 2010; Jackson and Carlson, 2011; Lightfoot et al., 1993; Storey et al., 1997; Thompson and Gibson, 2000). Some studies have also suggested that recycled crustal components were involved in CFB genesis, but such analyses have often been based on a limited number of chemical or physical variables (e.g., Cordery et al., 1997; Day, 2013; Gibson, 2002; Horan et al., 1995; Kent et al., 2002; Leitch and

Davies, 2001; Luttinen et al., 2010; Rocha-Júnior et al., 2012; Shirey, 1997; Sobolev et al., 2007).

The Jurassic Karoo large igneous province, located in southern Africa and Antarctica (Fig. 1), is a typical CFB province as it is characterized by basalts that are highly evolved and/or show strong geochemical affinity to the lithosphere (e.g., Ellam 2006; Hawkesworth et al. 1984; Jourdan et al. 2007; Luttinen and Furnes 2000; Luttinen et al 1998; Riley et al. 2005; Sweeney et al. 1994). This has led some researchers to propose that the Karoo CFB parental melts were generated solely within the Gondwanan lithosphere (e.g., Ellam and Cox, 1989; Jourdan et al., 2007). On the other hand, the high initial $^{187}Os/^{188}Os$ of some Karoo picrites indicate involvement of plume-like enriched mantle sources (Ellam et al., 1992). In addition, some recent studies in Antarctica (Fig. 1) have revealed several Karoo magma types that show isotopic and trace element characteristics indicative of sublithospheric sources (Heinonen and Luttinen, 2008, 2010; Heinonen et al., 2010, 2013; Luttinen et al., 1998; Riley et al., 2005). High-Mg dikes from the Vestfjella mountain range (Fig. 1) can be divided into depleted and enriched ferropicrite suites that show Sr, Nd, Pb, and Os isotopic compositions similar to those of Southwest Indian Ridge mid-ocean ridge basalts (SWIR MORBs) and ocean island basalts (OIBs), respectively (Heinonen et al., 2010). In addition, the Ahlmannryggen mountain range (Fig. 1) hosts a previously recognized suite of mafic and ultramafic dikes (Group 3 of Riley et al., 2005) that crosscut Precambrian basement and are characterized by notably high ε_{Nd} (from +5 to +9 at 180 Ma) and MgO (8–22 wt. %) indicating their crystallization from primitive melts derived from sublithospheric sources (Riley et al., 2005). They also show slightly elevated $^{87}Sr/^{86}Sr$ (0.7035–0.7062 at 180 Ma) and geochemical (low CaO and high Ti and Zn/Fe) and mineral chemical (high-Ni olivine) evidence for derivation from pyroxenite-bearing sources (Riley et al., 2005; Heinonen et al., 2013).

High-Mg rocks related to CFBs are rare but important carriers of petrogenetic information on the sources and origin of these massive volcanic phenomena. In this study, we present Pb and Os isotopic data on the Group 3 dikes of Ahlmannryggen and, in conjunction with previously published major element, trace element, mineral chemical, and Sr and Nd isotopic data, evaluate the role of lithospheric contamination on their parental magmas and attempt to decipher the composition and nature of their mantle sources. Finally, we evaluate the implications of our findings in relation to Karoo magmatism, and to CFB magmatism in general.

2. Geological and geochemical context

The Karoo CFBs erupted on the landmasses of Africa and Antarctica, both then part of the Gondwana supercontinent, at 184–178 Ma (Fig. 1; Jourdan et al., 2005). The magmas intruded through thick continental lithosphere that consists of a variety of Archean to Paleozoic rocks.

2.1 Pre-Jurassic geology of western Dronning Maud Land

In western Dronning Maud Land, the NW portion of the area is dominated by the Archean Grunehogna craton (Fig. 1; Krynauw et al., 1991; Wolmarans and Kent, 1982). The Archean basement is only exposed at Annandagstoppane (Fig. 1; Marschall et al., 2010) and elsewhere is covered by metamorphosed Mesoproterozoic supracrustal rock types belonging to the Ritscherflya Supergroup and/or by Borgmassivet mafic intrusions (Krynauw et al., 1988, 1991; Riley and Millar, in press; Wolmarans and Kent, 1982). The southern and eastern parts of the Precambrian basement of western Dronning Maud Land belong to the Proterozoic Maud Belt (Fig. 1; Groenewald et al., 1995). Late Paleozoic sedimentary rocks that overlay the basement are exposed at Vestfjella, Heimefrontfjella, and southwest Kirwanveggen (Fig. 1; e.g., Juckes, 1972; Wolmarans and Kent, 1982).

2.2. The Karoo CFBs and related intrusive rocks of Antarctica

The Karoo CFBs, exposed at Vestfjella, Kirwanveggen, and Heimefrontfjella, represent the youngest preserved rock unit at western Dronning Maud Land (Fig. 1). Associated intrusive rocks are more widespread and can also be found crosscutting the basement at Ahlmannryggen, Mannefallknausane, and H. U. Sverdrupfjella (Fig. 1). The mafic to ultramafic CFBs and intrusive rocks show notable geochemical heterogeneity and can be grouped into various low-Ti and high-Ti magma types in terms of their trace element and isotopic composition (Luttinen and Furnes, 2000; Luttinen et al., 2010; Riley et al., 2005). Unlike from the African parts of the Karoo CFB province, several dikes of unusual sublithospheric geochemical character have been described from Antarctica: the Sr, Nd, Pb, and Os isotopic compositions of the Vestfjella depleted ferropicrite suite (Fig. 2; Heinonen and Luttinen, 2008, 2010) are indistinguishable from those of SWIR MORBs and imply derivation from an upper mantle source (Heinonen et al., 2010), although non-chondritic primitive mantle sources may also be plausible (Jackson and Carlson, 2011). Incompatible element depleted low-Nb basaltic and picritic dikes also identified from Vestfjella have been interpreted to represent low-pressure, high-degree melting of this same source (Heinonen et al., 2010). The OIB-like Vestfjella enriched ferropicrite suite (Fig. 2; Heinonen and Luttinen, 2008) has been ascribed to either an anomalous lithospheric source or a recycled sediment-influenced pyroxenite mantle source (Heinonen et al., 2010). The depleted Group 3 dikes from Ahlmannryggen are considered in more detail in the following section.

2.2.1 Group 3 dikes of Ahlmannryggen

The Karoo dikes of Ahlmannryggen crosscut the Precambrian Ritscherflya metasupracrustal rocks and can be grouped into four geochemical types (Groups 1–4; Riley et al., 2005). Most of the dikes are fairly evolved basalts, but Group 3 and Group 4 include several samples with high MgO (> 8 wt. %). Whereas Group 4 exhibits relatively unradiogenic ε_{Nd} (from -5 to +2 at 180 Ma), Group 3 shows highly radiogenic ε_{Nd} (from +5 to +9 at 180 Ma) indicative of derivation from sublithospheric sources (Fig. 2). The Group 3 dikes show only negligible secondary alteration (e.g., average LOI = 1 wt. %) and are generally porphyritic with olivine and/or pyroxene (orthopyroxene and/or augite) phenocrysts surrounded by groundmass consisting of pyroxene, plagioclase, and Fe-Ti oxides. The olivine phenocrysts show Mg-rich ($Fo_{76–90}$) compositions indicating that the dikes crystallized from primitive magmas (Heinonen et al., 2013).

The Group 3 dikes are characterized by high FeO_{tot} (12–14 wt. %) and TiO_2 (3.3–4.9 wt. %), low CaO (9–11 wt. %), La/Sm (0.5– 0.8 chondrite-normalized), and Nb/Y (0.1–0.3), high ε_{Nd} (from +5 to +9), and slightly elevated $^{87}Sr/^{86}Sr$ (0.7035–0.7062) at 180 Ma (Table 1; Fig. 2; Riley et al., 2005). They also show general depletion of strongly incompatible elements, and depletion of large-ion lithophile elements (LILE), U, and Th relative to Nb and Ta. The dikes are not significantly altered and LILEs (and $^{87}Sr/^{86}Sr$) show coherent behaviour with more immobile elements in general, indicating that post-crystallization modification has been negligible (cf. Riley et al., 2005).

Group 3 dikes were further divided into two subgroups on the basis of Sr and Nd isotopic composition (Fig. 2) by Riley et al. (2005): the high-ε_{Nd} subgroup (ε_{Nd} = from +7.0 to +9.0 and $^{87}Sr/^{86}Sr$ = 0.7035–0.7041 at 180 Ma) was thought to have crystallized from uncontaminated mantle-derived magmas whereas the composition of the low-ε_{Nd} subgroup (ε_{Nd} = from +5.0 to +5.5 and $^{87}Sr/^{86}Sr$ = 0.7054–0.7062 at 180 Ma) was thought have been affected by minor contamination with continental crust (possibly Precambrian Borgmassivet intrusions; Riley et al., 2005). The subgroups are spatially separated by a distance of ~20 km (Fig. 1).

Riley et al. (2005) hypothesized that the Group 3 magmas represent partial melts of a strongly depleted mantle component possibly entrained in a mantle plume. Recently, Heinonen et al. (2013) interpreted the overall geochemical (high Ti, low Ca) and mineral chemical (high-Ni olivine) characteristics of the dikes to indicate a significant role for pyroxene-rich sources in their petrogenesis. Ar-Ar whole-rock data indicate a disturbed and thus somewhat unreliable plateau age of 187.3 ± 3.6 Ma (sample Z1816.1; Riley et al., 2005). More detailed information on the Group 3 and other Jurassic Ahlmannryggen dikes and their comparisons with other Karoo CFBs are provided in Riley et al. (2005) and Heinonen et al. (2013).

3. Sample selection and analytical methods

Nine Group 3 samples from distinct dike outcrops were selected for Pb and Os isotopic analyses (Table 1). The isotopic measurements were performed at the Department of Terrestrial Magnetism (DTM) of the Carnegie Institution of Washington. The rock samples were extracted with a hammer from the bedrock and subsequently chopped to smaller pieces with a hydraulic press and by hammering the samples under a cloth. Sample pieces that had metal marks on them or were in direct contact with the press were not included. The samples were further crushed in a ceramic jaw crusher and the resulting chips were hand-picked and powdered in an agate or ceramic mill to further avoid contamination with metals. The crushing devices were purified with aliquots of clean quartz between runs. For the chemical treatment of Pb and Os at the DTM, the reader is referred to Heinonen et al. (2010) with exceptions that are listed in Table S1.

Isotopic compositions of Pb and Re for isotope-dilution concentration determinations were measured on the DTM multiple-collector Nu Plasma high resolution inductively coupled plasma mass spectrometer (HR ICP-MS). Pb was measured statically using Faraday cups. Mass fractionation was corrected by comparing bracketing runs of the NBS-981 standard to values reported by Todt et al. (1996). Four standard runs gave the following average isotopic ratios: $^{206}Pb/^{204}Pb = 16.937 \pm 0.005$ (2σ), $^{207}Pb/^{204}Pb = 15.491 \pm 0.005$, and $^{208}Pb/^{204}Pb = 36.70 \pm 0.01$. The uncertainty for Pb for the sample analyses is assigned the external errors measured for the multiple standard analyses, because they are larger than the in-run precisions. The low Re concentrations were measured by simultaneous collection in electron multipliers. Instrument fractionation for Re was estimated by normalizing to bracketing standard runs. Analytical precision for Re is estimated to be 3 %.

The isotopic composition of Os was measured by thermal ionization mass spectrometry (TIMS) using the Thermo-Fisher Triton of DTM. Osmium was loaded on Pt filaments, covered with $Ba(OH)_2$ and run as OsO_3^- ions. The measurements were obtained on the single electron multiplier, monitoring interferences from Re, and correcting for fractionation to $^{192}Os/^{188}Os = 3.083$. Four intervening in-house standard (DTM Johnson Matthey Os) runs gave an average $^{187}Os/^{188}Os$ ratio of 0.17381 ± 0.00004 (2σ). The uncertainty for Os is assigned to the in-run precisions, because they are larger than the external error.

The extraction techniques and mass spectrometry resulted in total blanks of 100 pg for Pb and < 2 pg for Re and Os that posed negligible corrections for concentrations and isotopic ratios in all cases.

4. Results

Pb and Os isotopic data for the Ahlmannryggen Group 3 dikes are shown in Table 1 and illustrated in Figs. 3 and 4. Hereafter, the $^{206}Pb/^{204}Pb$, $^{207}Pb/^{204}Pb$, $^{208}Pb/^{204}Pb$, and $^{187}Os/^{188}Os$ (and $^{87}Sr/^{86}Sr$ and ε_{Nd}) of the Ahlmannryggen dikes and other Karoo CFB-related rocks refer to initial ratios calculated at 180 Ma unless otherwise stated. The radiogenic ingrowth of Pb was calculated using U and Th concentration data from Riley et al. (2005).

4.1. Pb and Os isotopic composition of Group 3 dikes

The high-ε_{Nd} subgroup shows a wide range of Pb isotopic compositions ($^{206}Pb/^{204}Pb$ = 17.4–18.4, $^{207}Pb/^{204}Pb$ = 15.3–15.5, and $^{208}Pb/^{204}Pb$ = 37.0–37.9). The three samples with the most radiogenic ε_{Nd} (+9) are the most radiogenic also in terms of Pb isotopic ratios: $^{206}Pb/^{204}Pb$ of 18.4 is the highest recorded for Karoo CFBs and related intrusive rocks (Fig. 3). The $^{206}Pb/^{204}Pb$ and $^{207}Pb/^{204}Pb$ of these three samples are similar to those found in some SWIR MORB (Fig. 3c), but $^{208}Pb/^{204}Pb$ is lower (and ε_{Nd} higher) at a given $^{206}Pb/^{204}Pb$ (Fig. 3d). Their $^{206}Pb/^{204}Pb$ and $^{207}Pb/^{204}Pb$ (and $^{87}Sr/^{86}Sr$ and ε_{Nd}) are also rather similar to the prevalent mantle component (PREMA) of Zindler and Hart (1986). The low-ε_{Nd} subgroup shows a more restricted range of Pb isotopic compositions ($^{206}Pb/^{204}Pb$ = 17.7–17.8, $^{207}Pb/^{204}Pb$ = 15.4, and $^{208}Pb/^{204}Pb$ = 37.4–37.5) that overlap those of the Karoo CFBs.

The Os isotopic composition correlates negatively with ε_{Nd}: the high-ε_{Nd} subgroup shows $^{187}Os/^{188}Os$ (0.124–0.125) akin to DMM, whereas the low-ε_{Nd} subgroup shows marginally higher $^{187}Os/^{188}Os$ of 0.127–0.128 (Fig. 4).

5. Discussion

5.1. Crustal contamination of Group 3 magmas

The high-ε_{Nd} subgroup exhibits the highest ε_{Nd} values (up to +9.0) recorded for Karoo CFBs, suggesting that their primary melts were generated in the sublithospheric mantle. Samples with the highest ε_{Nd} show elevated $^{87}Sr/^{86}Sr$ and $^{206}Pb/^{204}Pb$ relative to DMM at 180 Ma (Fig. 3). These are considered primary features (and not caused by in-situ reactions with wall rock or hydrothermal alteration), because $^{87}Sr/^{86}Sr$ and $^{206}Pb/^{204}Pb$ correlate negatively with, e.g., Th/Ta and La/Nb, and because the samples having ε_{Nd} of +9 exhibit homogeneous compositions in terms of mobile trace elements and Sr and Pb isotopic ratios (cf. Riley et al., 2005). In the case of secondary alteration, distinct samples from different dikes would not be expected to form such coherent compositional groups (cf. Fig. 2 and 3).

The new Pb isotopic data reveal two possible contamination trends for the Group 3 dikes: (1) The high-ε_{Nd} subgroup shows a rather wide range of Pb isotopic compositions that correlate negatively with $^{87}Sr/^{86}Sr$ and positively with ε_{Nd} (Fig. 5); (2) The low-ε_{Nd} subgroup exhibits relatively lower ε_{Nd} and higher $^{87}Sr/^{86}Sr$ at a given $^{206}Pb/^{204}Pb$ (Fig. 5). Importantly, the relatively high $^{187}Os/^{188}Os$ of the low-ε_{Nd} subgroup (Fig. 4), and the Nd-Pb isotope systematics of the high-ε_{Nd} subgroup (Fig. 5b; trend not directed towards the lithosphere-signatured CFBs) make SCLM an unlikely contaminant in both cases.

In order to constrain crustal contamination of Group 3 dikes, we performed energy-constrained assimilation-fractional crystallization (EC-AFC) modeling (Bohrson and Spera, 2001; Spera and Bohrson, 2001) using a primitive high-ε_{Nd} sample Z1816.2 as a parental melt composition and a diverse suite of Archean Kaapvaal TTGs, shales, and amphibolites (Kreissig et al., 2000), and Proterozoic Ritscherflya sedimentary rocks (Moyes et al., 1995; Pb after Wareham et al., 1998), Maud Belt gneisses (H.U. Sverdrupfjella; Wareham et al., 1998), and Borgmassivet mafic intrusive suite (Sr and Nd data after the model of Riley et al., 2005; Pb data by T.R. Riley, unpublished) as contaminants. Details of the contamination modeling are presented in Table S2.

Our EC-AFC modeling indicates that minor (~1 %) contamination of a high-ε_{Nd} parental magma with an Archean crustal contaminant could plausibly explain the Sr, Nd, and Pb isotopic composition of the three samples that belong to the high-ε_{Nd} subgroup and show ε_{Nd} of +7 and relatively unradiogenic Pb isotopic compositions (Fig. 5; cf. Table 1). The low-ε_{Nd} subgroup, on the other hand, has overly high $^{87}Sr/^{86}Sr$ and low ε_{Nd} at a given $^{206}Pb/^{204}Pb$ to be explained by contamination of a high-ε_{Nd} parental magma with most of the Archean crustal components (Fig. 5); an anomalous TTG contaminant (sample 96/228) is able to produce similar $^{87}Sr/^{86}Sr$, ε_{Nd}, and $^{206}Pb/^{204}Pb$ at ~1 % of contamination, but cannot explain the higher $^{207}Pb/^{204}Pb$ and $^{208}Pb/^{204}Pb$ of the low-ε_{Nd} subgroup (Fig. 5). Models with felsic Proterozoic contaminants (H. U. Sverdrupfjella gneiss and Ritscherflya sedimentary rock) show a slightly better fit in terms of $^{87}Sr/^{86}Sr$, ε_{Nd}, $^{206}Pb/^{204}Pb$, and $^{208}Pb/^{204}Pb$, but are not compatible with the lower $^{207}Pb/^{204}Pb$ of the low-ε_{Nd} subgroup. Based on our model, the Borgmassivet intrusive suite with relatively high $^{206}Pb/^{204}Pb$ also appears to be an unsuitable contaminant.

Although the Sr, Nd, and Pb isotopic composition of the low-ε_{Nd} subgroup cannot be satisfactorily explained by contaminating a high-ε_{Nd} parental magma with aforementioned crustal materials, our modeling is hampered by the lack of Pb data on the Proterozoic contaminants (e.g., H.U. Sverdrupfjella and Borgmassivet models based only on a single analysis), and such a scenario cannot be completely ruled out. The spatially distinct high-ε_{Nd} and low-ε_{Nd} subgroups may thus have fractionated in separate magma chambers at different crustal levels (cf. Fig. 1). On the other hand, the higher olivine Ni contents and $^{187}Os/^{188}Os$ (Fig. 4) of the low-ε_{Nd} subgroup imply that their parental magmas may in fact have been compositionally distinct from the high-

ε_{Nd} parental magmas (e.g., derive from more pyroxene-rich sources; Heinonen et al., 2013; cf. section 5.2.3).

Given the likelihood of Archean crustal contamination in the case of the high-ε_{Nd} samples with ε_{Nd} of +7 and the possibility of either Archean or Proterozoic crustal contamination combined with source heterogeneity in the case of the low-ε_{Nd} subgroup, we concentrate on the three uncontaminated high-ε_{Nd} samples (Z1812.3, Z1816.1, and Z1816.2 with ε_{Nd} of +9) in the following discussion on Group 3 mantle sources.

5.2. Sublithospheric mantle sources of the Group 3 dikes

5.2.1. Evidence for a pyroxene-rich source and its origin

The major element and mineral chemical characteristics of the Group 3 dikes, discussed in detail by Riley et al. (2005) and Heinonen et al. (2013), provide evidence for contribution from pyroxenite sources. Summarizing, picrites with such high TiO_2 (3–5 wt. %) and FeO_{tot} (12–14 wt. %) and low CaO (9–11 wt. %) cannot derive from melting of solely peridotitic mantle (Heinonen et al., 2013; cf. Herzberg and Asimow, 2008; Prytulak and Elliott, 2007; Tuff et al., 2005). The high Ni contents in olivine (0.5–0.6 wt. % at Fo_{90}) and high whole-rock Zn/Fe ($1.2– 1.5 \cdot 10^{-3}$) are also indicative of pyroxene-rich sources (Heinonen et al., 2013; cf. Le Roux et al., 2010; Sobolev et al., 2007), although the former may also partly reflect high pressures beneath the Gondwanan lithosphere (cf. Li and Ripley, 2010). Importantly, the negative correlation of whole-rock CaO (at a given MgO) and olivine Ni point to primary compositional variation that is compatible with some degree of mixing of pyroxenitic and peridotitic source components (Heinonen et al., 2013).

The pyroxene content of a mantle section can be influenced by local-to-regional scale melt infiltration and metasomatism in the lithospheric mantle (e.g., Bodinier et al., 2008; Liu et al., 2005) or by reactions between mantle peridotite and partial melts of subducted oceanic crust (e.g., Mallik and Dasgupta, 2012; Yaxley and Green, 1998). The low La/Sm and highly radiogenic Nd isotopic signature of the high-ε_{Nd} subgroup (Fig. 6 and 7) are not readily explained by melting of metasomatized lithospheric mantle (e.g., Obata and Nagahara, 1987) that is expected to be relatively enriched in the most incompatible elements and develop relatively unradiogenic ε_{Nd} over time. On the other hand, lithospheric mantle pyroxenites with strongly depleted incompatible trace element compositions have been reported from, e.g., the Ronda orogenic peridotite (e.g., Bodinier et al., 2008). These pyroxenites show strong relative depletion of Nb and Ta (e.g., Bodinier et al., 2008; Garrido and Bodinier, 1999), however, and thus cannot be a primary source for the high-ε_{Nd} subgroup that shows enrichment of Nb and Ta relative to similarly incompatible elements (cf. Fig. 6).

Oceanic crust generally exhibits low Sm/Nd and would thus also develop relatively low ε_{Nd} over time, unless it had been modified by, e.g., dehydration and/or partial melting related to subduction (e.g., Kogiso et al., 1997; Sakuyama et al., 2013), and does not contain significant amounts of pelagic sediments (Fig. 7; Stracke et al., 2003; cf. Plank and Langmuir, 1998). Given that convergent-margin processing of subducted crust is a widely recognized process, Nd may be up to three times more mobile in subduction fluids than Sm (Kogiso et al., 1997), and fluid-immobile Nb and Ta are effectively held in subducted igneous oceanic crust (Kogiso et al., 1997; cf. Rudnick et al., 2000), we conclude that Group 3 pyroxenite sources most likely contained recycled igneous crustal materials. The nature and significance of this recycled component is evaluated in detail in the following sections.

5.2.2. Trace element constraints on the recycled mantle component

In order to model the trace element composition of the recycled component, we used the mean MORB of Gale et al. (2013) as the igneous crust composition. The effects of subduction modification were calculated on the basis of fluid-rock distribution coefficients obtained in dehydration experiments on a MORB-like amphibolite (Kogiso et al., 1997; Table S3). Such a completely modified recycled MORB is referred to as sm-MORB 1, whereas a more mildly (50% less effectively) modified recycled MORB is referred to as sm-MORB 2 (Fig. 6). The high-ε_{Nd} signature shows a better fit with the sm-MORB 2 component (especially in the case of Pb; Fig. 6) and thus we concentrate on it in the following discussion.

The trace element pattern of sm-MORB 2 (10%) + DMM peridotite (90%) mixture illustrates that a subduction-modified signature is effectively transferred to the ambient mantle even at low portions of entrained recycled material due to low incompatible element contents of DMM (Fig. 6). Furthermore, partial melt model of the mixture indicates that such a source is capable of producing a melt with trace element characteristics akin to the high-ε_{Nd} subgroup (Fig. 6). The positive Ba anomaly and more incompatible-element-depleted trace element pattern of the high-ε_{Nd} subgroup relative to the model could be related to an additional Ba-rich component (or lower mobility of Ba during subduction) and more depleted compositions of the crustal and/or mantle components than those used in the model, respectively. Nevertheless, given the overall similarities (Fig. 6), we suggest that the incompatible trace element signature of the high-ε_{Nd} subgroup can be viably explained by sources that contain subduction-modified MORB.

5.2.3. Isotopic constraints on the recycled mantle component

In order to model the Sr, Nd, and Pb isotopic composition of the recycled MORB component (cf. section 5.2.2.), we used the spreadsheet and standard input parameters provided by Stracke et al. (2003). Due to uncertainties related to initial concentrations, isotopic compositions and behaviour of Re and Os (Carlson, 2005; Stracke et al., 2003), Os isotopes were modeled by

simple binary mixing of DMM and MORB, compositions of which were constrained on the basis of data compilations presented in Shirey and Walker (1998). We emphasize that all the model parameters represent average or recommended values; full details of the modeling are presented in Fig. 7 and 8, and in Table S4.

Modeling of isotopes provides further constraints on the petrogenesis of Group 3 dikes (Fig. 7). Using recommended values for the isotopic evolution of the mantle and crustal components (Table S4; cf. Stracke et al., 2003), the best-fit in terms of Nd and Pb isotopic compositions is attained with a mixture of 0.7 Ga recycled sm-MORB 2 (~10–30 %) and DMM (~80–90 %) (Fig. 7). In the case of Nd isotopes, an even better fit would be attained with a more depleted DMM (cf. Workman and Hart, 2005) or MORB composition (cf. Gale et al., 2013) or if Nd is assumed to be more mobile during subduction (cf. grey curve with sm-MORB 1 component in Fig. 7). The high $^{87}Sr/^{86}Sr$ of the high-ε_{Nd} subgroup suggests that the Sr isotopic signature of the recycled component was more radiogenic than in our model (Fig. 7a). Radiogenic Sr is readily introduced into the upper oceanic crust via replacement by seawater Sr (30% on average; Kawahata et al., 1987) that has also been incorporated into the equations of Stracke et al. (2003). Seawater-influenced (30%) Sr isotope model is compatible with trace element and Nd and Pb isotope models (cf. Fig. 6 and 7).

For comparison, models with unmodified recycled MORB, additional sedimentary component, as well as pervasively fluid-modified MORB (sm-MORB 1) fail to produce the Sr, Nd, and Pb isotopic composition of the uncontaminated high-ε_{Nd} subgroup (Fig. 7). Although, the model with sm-MORB 1 produces a better-fit for ε_{Nd} than the model with sm-MORB 2, Sr shows a poor fit even with seawater Sr included. Furthermore, a model with sm-MORB 1 shows radiogenic Pb isotopic composition that would constrain the amount of recycled crust to be less than 2% in the mixture. Such a small portion of recycled component would not be enough to produce the pyroxenite fingerprint observed in the major element geochemistry of the Group 3 dikes (Heinonen et al., 2013).

The low $^{187}Os/^{188}Os$ of the high-ε_{Nd} subgroup (Fig. 4) is not directly compatible with recycled crustal sources. Recycled MORB sources should develop high $^{187}Os/^{188}Os$ over time (> 0.13; e.g., Carlson and Nowell, 2001; Carlson et al., 2006; Day et al., 2009; Sobolev et al., 2008), because MORBs exhibit high Re (0.5–2 ppb) and low Os (0.001–0.05 ppb) relative to depleted mantle peridotite (0.05–0.14 ppb and 0.8–9 ppb, respectively; Shirey and Walker, 1998). In the case of a mixed source, however, the Os-rich peridotite component will control the Os isotopic composition (e.g., Shirey and Walker, 1998), unless the MORB component is old (≥ 2 Ga) or constitutes a major fraction of the mixture. Importantly, the high Os contents of the high-ε_{Nd} subgroup (1–2 ppb; Table 1) require a predominantly peridotitic source and our Sr, Nd, and Pb isotopic modeling suggests that the recycled component must have been quite young (< 1 Ga; cf. section 5.2.4). In addition, studies of subducted portions of oceanic crust (i.e. eclogites and

blueschists; Becker, 2000; Dale et al., 2007) have indicated Os to be relatively immobile and Re relatively mobile (similar to Rb, Ba, and K; Dale et al., 2007) during subduction-related dehydration of the basaltic oceanic crust. Therefore, subduction-related loss of Re would tend to decrease the radiogenic production of ^{187}Os in a mixed mantle source. Our mixing models demonstrate that the Os isotopic composition is indeed highly dependent on the Os content of the peridotite component and that the effect of possible Re loss is negligible (Fig. 8). The Os isotopic composition of the high-ε_{Nd} subgroup can be best explained by melting of a mixture of Os-rich DMM (~70− 90%) and Re-poor MORB (~10− 30%; Fig. 8, models A and B) that is compatible with the trace element and Sr, Nd, and Pb isotopic modeling (cf. Fig. 6 and 7).

5.2.4. Constraints on the age of the recycled mantle component

We emphasize that the recycling age (i.e. the age at which the recycled crust started to evolve as a closed system until melting at 180 Ma; cf. Stracke et al., 2003) of 0.7 Ga suggested by our isotopic models (Fig. 7 and 8) should not be considered definitive given all the possible uncertainties in model parameters. Nevertheless, the recycled component is not likely to be older than 1.0 Ga, because such a component would result in low ε_{Nd} and would require higher input of seawater Sr to produce the high-ε_{Nd} signature at a given Pb isotopic composition (Fig. 7). In addition, due to the greater divergence in isotopic composition with time, the amount of ≥1 Ga recycled component in the mixture would have to be significantly below 10% for it to result in high-ε_{Nd} signature (Fig. 7). This would not likely be enough to produce the pyroxenite fingerprint observed in the major element geochemistry of the Group 3 dikes (Heinonen et al., 2013). The aforementioned effects of recycling age are not significantly affected by reasonable modifications in the other model parameters and, therefore, we conclude that the Group 3 dikes sampled a recycled component that was less than 1 Ga old.

5.2.5. Nature of the peridotitic mantle component

We used DMM as the peridotitic source component in the trace element and isotopic modeling (Fig. 6–8), because its composition is relatively well constrained (Workman and Hart, 2005). This depleted peridotite component could also represent the mantle portion of the subducted oceanic lithosphere, which would be difficult to distinguish geochemically from DMM if mixed with recycled crustal sources. As an alternative, Jackson and Carlson (2011) recently suggested that CFBs could derive from non-chondritic primitive mantle sources that had remained untapped deep in the Earth's mantle for over 4 Ga. Their primary arguments were related to the isotopic characteristics of primitive CFBs: many of them exhibit high ^{3}He/^{4}He, non-chondritic primitive mantle-like ε_{Nd} (+5 to +9 at present), and Pb isotopic compositions that plot near the geochron in ^{207}Pb/^{204}Pb vs. ^{206}Pb/^{206}Pb space (Fig. 7). Jackson and Carlson (2011) further suggested that the PREMA component that seems to dominate in OIB sources (Zindler and Hart,

1986) and closely corresponds to the isotopic composition of the uncontaminated high-ε_{Nd} subgroup (Fig. 7) could represent mixing of non-chondritic primitive mantle with recycled materials.

It is difficult to distinguish between DMM and non-chondritic primitive mantle peridotite source without He isotopic data (cf. Fig. 7). Using the most recently reported trace element compositions for the peridotite components, we modeled the partial melting of mixtures consisting of DMM (Workman and Hart, 2005) or non-chondritic primitive mantle (Jackson and Jellinek, 2013) and subduction-modified MORB (sm-MORB 2; cf. Fig. 6). The most notable differences between the modeled melts are the positive Pb anomaly and relative enrichment in the most incompatible elements in the case of the non-chondritic primitive mantle mixture (Fig. 9). Given that formation of mantle pyroxenite is a complex process involving several mineral-melt reactions (e.g., Bodinier et al., 2008; Mallik and Dasgupta, 2012), Pb is the most mobile of the concerned elements during subduction (cf. Fig. 6), and that the overall shape of the trace element signature is dependent on melting conditions, it is difficult to uniquely identify the peridotite component entrained in Group 3 dikes on the basis of trace element compositions. If the peridotitic component is non-chondritic primitive mantle, it would have to be from the high-ε_{Nd} compositional end of the spectrum proposed for this component (cf. Fig. 7b).

5.3. Group 3 sources and CFB magmatism

The compositions of the Ahlmannryggen Group 3 dikes provide evidence for the involvement of a recycled MORB component in Karoo magmatism. In addition, sediment-bearing recycled sources have been suggested for the Vestfjella enriched ferropicrite suite (Heinonen et al., 2010). Interestingly, isotopic models imply similar recycling ages in both cases (best-fit at 0.7 and 0.8 Ga, respectively; Fig. 7; Heinonen et al., 2010). At ~0.7–1.0 Ga, oceanic crust was being subducted along the margins of the supercontinent Rodinia (e.g., Murphy et al., 2004). Whether the subducted crust remained in the upper mantle or was recycled via lower mantle and entrained by a deep-seated mantle plume before being incorporated into the sources of the Karoo CFBs is unclear (cf. Heinonen et al., 2010). Although the suggested recycling ages are compatible with both options (cf. Sobolev et al., 2011a), we consider that whole-mantle circulation of the oceanic crust would probably have led to a series of metamorphic and melting events causing strong compositional modifications in the subducted material, whereas our models infer that the compositional effects of the recycling process were limited to subduction modification (Fig. 6– 8). We therefore suggest that the purported recycled components rather resided in the upper mantle and were entrained into a rising mantle plume (cf. Richards et al., 1989; Riley et al., 2005; scenario 2 of Jourdan et al., 2007) or were heated within the ambient depleted upper

mantle beneath the insulating Gondwana supercontinent (cf. Coltice et al., 2009; Hastie et al., 2014; Heinonen et al., 2010; scenario 1 of Jourdan et al., 2007).

The role of lithospheric sources in the generation of the Karoo CFBs is another outstanding question (cf. Heinonen et al., 2010; Jourdan et al., 2007; Luttinen et al., 2010). Importantly, the Sr-Nd isotopic compositions of the Karoo CFBs can be reproduced by lithospheric contamination of melts derived from DMM sources (cf. Fig. 2; Heinonen et al., 2010). In contrast, the Group 3 high-ε_{Nd} dikes with high $^{87}Sr/^{86}Sr$ appear to be unsuitable to represent parental magmas for the majority of the Karoo CFBs (cf. Fig. 2), implying that their sources did not have a major role in Karoo magmatism. The anomalous geochemical signature of the high-ε_{Nd} subgroup does not exclude the possibility that Karoo CFBs carry geochemical traces of *some other* recycled components, however. For example, less intensive subduction-modification or seawater alteration, or additional sedimentary component in the recycled crust would lead to less radiogenic ε_{Nd} in the recycled component (cf. Fig. 7). Such a mild fingerprint, combined with the effect of additional contamination with the continental lithosphere, would be difficult to distinguish from the jungle of common CFB signatures (cf. low-ε_{Nd} subgroup; Fig. 5 and 7). Accordingly, our results lend support to the possibility that the lithospheric geochemical signature typical of most CFBs could have been inherited at least partly from *recycled* lithospheric materials that melted in the deep mantle. Similar conclusions have recently been drawn from geochemical and isotopic data (Ewart et al., 2004; Luttinen et al., 2010; Rocha-Júnior et al., 2012), olivine and melt inclusion chemistry (Kent et al., 2002; Sobolev et al., 2007), and geophysical modeling (Cordery et al., 1997; Leitch and Davies, 2001) of CFBs. Our study substantiates the view that the potential of recycled sources in creating chemical heterogeneity of CFBs should be carefully assessed in every case.

6. Conclusions

Lead and Os isotopic data and previously published geochemical data for the Ahlmannryggen mafic and ultramafic dikes (Group 3) from the Antarctic extension of the Jurassic Karoo CFB province provide a geochemical window into the deep mantle beneath the Gondwana supercontinent. The radiogenic initial ε_{Nd} of the Group 3 dikes (from +5 to +9 at 180 Ma) indicates that their source was in the sublithospheric mantle. Correlations of Sr, Nd, and Pb isotopes indicate that some of the Group 3 magmas experienced minor contamination with continental crust. The Group 3 dikes that show the most radiogenic ε_{Nd} (+9) and derive from least contaminated magmas exhibit relatively radiogenic initial $^{206}Pb/^{204}Pb$ (18.2–18.4) and $^{87}Sr/^{86}Sr$ (0.7035–0.7037), indicating that they did not originate solely from ambient depleted upper mantle source ($^{206}Pb/^{204}Pb$ = 18.0 and $^{87}Sr/^{86}Sr$ = 0.7026 at 180 Ma). Isotopic and trace element

modeling indicates that the source contained ~10–30% of seawater-altered and subduction-modified MORB that was affected by the loss of LILEs, U, Th, Pb, LREE, Nd, and possibly Re, and had an recycling age of ≤ 1.0 Ga. This pyroxenitic component was entrained in an Os-rich peridotite matrix that either represents depleted mantle –like material (ambient upper mantle or recycled oceanic mantle lithosphere) or non-chondritic primitive mantle. Although the recycled MORB sources suggested for the Group 3 dikes were not likely the predominant source of Karoo magmatism, broadly similar but less subduction-modified or more sediment-influenced recycled components would not be readily recognized in evolved CFBs. Therefore, the role of recycled source components in influencing magma chemistry and petrogenesis in Karoo and other CFB provinces should be carefully assessed.

Acknowledgements

Dr. James Day and an anonymous reviewer provided constructive reviews and comments that improved the manuscript and strengthened the discussion. Dr. Timothy Mock from DTM helped in preparing the TIMS instrument for the analysis. The field and air operations staff at Halley Base during 2000–2001 are thanked for their support. Some of the diagrams have been produced with the help of the GCDkit software (Janoušek et al., 2006). Our research is funded by the Academy of Finland (Grant no. 252652).

Appendix A. Supplementary material

Supplementary material related to this article can be found from the attached file "SupplementaryData.xls".

References

Anderson, D.L., 2005. Large igneous provinces, delamination, and fertile mantle. Elements, 1, 271-275, http://dx.doi.org/ 10.2113/gselements.1.5.271

Beccaluva, L., Bianchini, G., Natali, C., Siena, F., 2009. Continental Flood Basalts and Mantle Plumes: a Case Study of the Northern Ethiopian Plateau. J. Petrol., 50, 1377-1403, http://dx.doi.org/10.1093/petrology/egp024

Becker, H., 2000. Re–Os fractionation in eclogites and blueschists and the implications for recycling of oceanic crust into the mantle. Earth Planet. Sci. Lett., 177, 287-300, http://dx.doi.org/10.1016/S0012-821X(00)00052-2

Bodinier, J., Garrido, C.J., Chanefo, I., Bruguier, O., Gervilla, F., 2008. Origin of Pyroxenite–Peridotite Veined Mantle by Refertilization Reactions: Evidence from the Ronda Peridotite (Southern Spain). J. Petrol., 49, 999-1025, http://dx.doi.org/10.1093/petrology/egn014

Bohrson, W.A., Spera, F.J., 2001. Energy-constrained open-system magmatic processes II: Application of energy-constrained assimilation-fractional crystallization (EC-AFC) model to magmatic systems. J. Petrol., 42, 1019-1041, http://dx.doi.org/10.1093/petrology/42.5.1019

Campbell, I.H., 2005. Large Igneous Provinces and the Mantle Plume Hypothesis. Elements, 1, 265-269, http://dx.doi.org/ 10.2113/gselements.1.5.265

Carlson, R.W., 2005. Application of the Pt-Re-Os isotopic systems to mantle geochemistry and geochronology. Lithos, 82, 249-272, http://dx.doi.org/10.1016/j.lithos.2004.08.003

Carlson, R.W., Czamanske, G.K., Fedorenko, V.A., Ilupin, I., 2006. A comparison of Siberian meimechites and kimberlites: implications for the source of high-Mg alkalic magmas and flood basalts. Geochem. Geophys. Geosyst., 7, http://dx.doi.org/10.1029/2006GC001342

Carlson, R.W., Lugmair, G.W., MacDougall, J.D., 1981. Columbia River volcanism: the question of mantle heterogeneity or crustal contamination. Geochim. Cosmochim. Acta, 45, 2483-2499, http://dx.doi.org/10.1016/0016-7037(81)90100-9

Carlson, R.W., Nowell, G.M., 2001. Olivine-poor sources for mantle-derived magmas: Os and Hf isotopic evidence from potassic magmas of the Colorado Plateau. Geochem. Geophys. Geosyst., 2, http://dx.doi.org/10.1029/2000GC000128

Coltice, N., Bertrand, H., Rey, P., Jourdan, F., Phillips, B.R., Ricard, Y., 2009. Global warming of the mantle beneath continents back to the Archaean. Gondwana Res., 15, 254-266, http://dx.doi.org/10.1016/j.gr.2008.10.001

Cordery, M.J., Davies, G.F., Campbell, I.H., 1997. Genesis of flood basalts from eclogite-bearing mantle plumes. J. Geophys. Res. B, 102, 20179-20197, http://dx.doi.org/10.1029/97JB00648

Corner, B., 1994. Geological evolution of western Dronning Maud Land within a Gondwana framework: Geophysics subprogramme. Final project report to SACAR. Department of Geophysics, Witwaterstrand University, South Africa, 21 p.

Dale, C.W., Gannoun, A., Burton, K.W., Argles, T.W., Parkinson, I.J., 2007. Rhenium–osmium isotope and elemental behaviour during subduction of oceanic crust and the implications for mantle recycling. Earth Planet. Sci. Lett., 253, 211-225, http://dx.doi.org/10.1016/j.epsl.2006.10.029

Day, J.M.D., 2013. Hotspot volcanism and highly siderophile elements. Chem. Geol., 341, 50-74, http://dx.doi.org/10.1016/j.chemgeo.2012.12.010

Day, J.M.D., Pearson, D.G., Hulbert, L.J., 2013. Highly siderophile element behaviour during flood basalt genesis and evidence for melts from intrusive chromitite formation in the Mackenzie large igneous province. Lithos, 182-183, 242-258, http://dx.doi.org/10.1016/j.lithos.2013.10.011

Day, J.M.D., Pearson, D.G., Macpherson, C.G., Lowry, D., Carracedo, J., 2009. Pyroxenite-rich mantle formed by recycled oceanic lithosphere: oxygen-osmium isotope evidence from Canary Island lavas. Geology, 37, 555-558, http://dx.doi.org/10.1130/G25613A.1

Eisele, J., Sharma, M., Galer, S.J.G., Blichert-Toft, J., Devey, C.W., Hofmann, A.W., 2002. The role of sediment recycling in EM-1 inferred from Os, Pb, Hf, Nd, Sr isotope and trace element systematics of the Pitcairn Hotspot. Earth Planet. Sci. Lett., 196, 197-212, http://dx.doi.org/10.1016/S0012-821X(01)00601-X

Elkins-Tanton, L.T., Hager, B.H., 2000. Melt intrusion as a trigger for lithospheric foundering and the eruption of the Siberian flood basalts. Geophys. Res. Lett., 27, 3937-3940, http://dx.doi.org/10.1029/2000GL011751

Ellam, R.M., 2006. New constraints on the petrogenesis of the Nuanetsi picrite basalts from Pb and Hf isotope data. Earth Planet. Sci. Lett., 245, 153-161, http://dx.doi.org/10.1016/j.epsl.2006.03.004

Ellam, R.M., Carlson, R.W., Shirey, S.B., 1992. Evidence from Re-Os isotopes for plume-lithosphere mixing in Karoo flood basalt genesis. Nature, 359, 718-721, http://dx.doi.org/10.1038/359718a0

Ellam, R.M., Cox, K.G., 1989. A Proterozoic lithospheric source for Karoo magmatism: evidence from the Nuanetsi picrites. Earth Planet. Sci. Lett., 92, 207-218, http://dx.doi.org/10.1016/0012-821X(89)90047-2

Ellam, R.M., Cox, K.G., 1991. An interpretation of Karoo picrite basalts in terms of interaction between asthenospheric magmas and the mantle lithosphere. Earth Planet. Sci. Lett., 105, 330-342, http://dx.doi.org/10.1016/0012-821X(91)90141-4

Ewart, A., Marsh, J.S., Milner, S.C., Duncan, A.R., Kamber, B.S., Armstrong, R.A., 2004. Petrology and Geochemistry of Early Cretaceous Bimodal Continental Flood Volcanism of the NW Etendeka, Namibia. Part 1: Introduction, Mafic Lavas and Re-evaluation of Mantle Source Components. J. Petrol., 45, 59-105, http://dx.doi.org/10.1093/petrology/egg083

Fram, M.S., Lesher, C.E., 1997. Generation and polybaric differentiation of East Greenland early Tertiary flood basalts. J. Petrol., 38, 231-275, http://dx.doi.org/10.1093/petroj/38.2.231

Gale, A., Dalton, C.A., Langmuir, C.H., Su, Y., Schilling, J., 2013. The mean composition of ocean ridge basalts. Geochem. Geophys. Geosyst., 14, http://dx.doi.org/10.1029/2012GC004334

Garrido, C.J., Bodinier, J.-L., 1999. Diversity of Mafic Rocks in the Ronda Peridotite: Evidence for Pervasive Melt–Rock Reaction during Heating of Subcontinental Lithosphere by Upwelling Asthenosphere. J. Petrol., 40, 729-754, http://dx.doi.org/10.1093/petroj/40.5.729

Gibson, S.A., 2002. Major element heterogeneity in Archean to Recent mantle plume starting-heads. Earth Planet. Sci. Lett., 195, 59-74, http://dx.doi.org/10.1016/S0012-821X(01)00566-0

Groenewald, P.B., Moyes, A.B., Grantham, G.H., Krynauw, J.R., 1995. East Antarctic crustal evolution: geological constraints and modelling in western Dronning Maud Land. Precambrian Res., 75, 231-250, http://dx.doi.org/10.1016/0301-9268(95)80008-6

Harris, C., Marsh, J.S., Duncan, A.R., Erlank, A.J., 1990. The petrogenesis of the Kirwan Basalts of Dronning Maud Land, Antarctica. J. Petrol., 31, 341-369, http://dx.doi.org/10.1093/petrology/31.2.341

Hastie, W.W., Watkeys, M.K., Aubourg, C., 2014. Magma flow in dyke swarms of the Karoo LIP: Implications for the mantle plume hypothesis. Gondwana Res., 25, 736-755, http://dx.doi.org/10.1016/j.gr.2013.08.010

Hawkesworth, C.J., Gallagher, K., Kelley, S., Mantovani, M., Peate, D.W., Regelous, M., Rogers, N.W., 1992. Parana magmatism and the opening of the South Atlantic. In: Storey, B.C., Alabaster, T., Pankhurst, R.J. (Eds.), Magmatism and the causes of continental break-up. Geological Society of London, London, United Kingdom (GBR), pp. 221-240, http://dx.doi.org/10.1144/GSL.SP.1992.068.01.14

Hawkesworth, C.J., Marsh, J.S., Duncan, A.R., Erlank, A.J., Norry, M.J., 1984. The role of continental lithosphere in the generation of the Karoo volcanic rocks: evidence from combined Nd- and Sr-isotope studies. In: Erlank, A.J. (Ed.), Petrogenesis of the volcanic rocks of the Karoo Province. Geological Society of South Africa, Special Publication 13, Johannesburg, South Africa (ZAF), pp. 341-354

Heinonen, J.S., Carlson, R.W., Luttinen, A.V., 2010. Isotopic (Sr, Nd, Pb, and Os) composition of highly magnesian dikes of Vestfjella, western Dronning Maud Land, Antarctica: A key to the origins of the Jurassic Karoo large igneous province? Chem. Geol., 277, 227-244, http://dx.doi.org/10.1016/j.chemgeo.2010.08.004

Heinonen, J.S., Luttinen, A.V., 2008. Jurassic dikes of Vestfjella, western Dronning Maud Land, Antarctica: Geochemical tracing of ferropicrite sources. Lithos, 105, 347-364, http://dx.doi.org/10.1016/j.lithos.2008.05.010

Heinonen, J.S., Luttinen, A.V., 2010. Mineral chemical evidence for extremely magnesian subalkaline melts from the Antarctic extension of the Karoo large igneous province. Miner. Petrol., 99, 201-217, http://dx.doi.org/10.1007/s00710-010-0115-9

Heinonen, J.S., Luttinen, A.V., Riley, T.R., Michallik, R.M., 2013. Mixed pyroxenite–peridotite sources for mafic and ultramafic dikes from the Antarctic segment of the Karoo continental flood basalt province. Lithos, 177, 366-380, http://dx.doi.org/10.1016/j.lithos.2013.05.015

Herzberg, C., Asimow, P.D., 2008. Petrology of some oceanic island basalts: PRIMELT2.XLS software for primary magma calculation. Geochem. Geophys. Geosyst., 9, http://dx.doi.org/10.1029/2008GC002057

Horan, M.F., Walker, R.J., Fedorenko, V.A., Czamanske, G.K., 1995. Osmium and neodymium isotopic constraints on the temporal and spatial evolution of Siberian flood basalt sources. Geochim. Cosmochim. Acta, 59, 5159-5168, http://dx.doi.org/10.1016/0016-7037(96)89674-8

Jackson, M.G., Carlson, R.W., 2011. An ancient recipe for flood-basalt genesis. Nature, 476, 316-319, http://dx.doi.org/10.1038/nature10326

Jackson, M.G., Jellinek, A.M., 2013. Major and trace element composition of the high $^{3}He/^{4}He$ mantle: Implications for the composition of a nonchonditic Earth. Geochem. Geophys. Geosyst., 14, 2954-2976, http://dx.doi.org/ 10.1002/ggge.20188

Janoušek, V., Farrow, C.M., Erban, V., 2006. Interpretation of Whole-rock Geochemical Data in Igneous Geochemistry: Introducing Geochemical Data Toolkit (GCDkit). J. Petrol., 47, 1255-1259, http://dx.doi.org/10.1093/petrology/egl013

Jourdan, F., Bertrand, H., Schaerer, U., Blichert-Toft, J., Féraud, G., Kampunzu, A.B., 2007. Major and trace element and Sr, Nd, Hf, and Pb isotope compositions of the Karoo large igneous province, Botswana-Zimbabwe: lithosphere vs mantle plume contribution. J. Petrol., 48, 1043-1077, http://dx.doi.org/10.1093/petrology/egm010

Jourdan, F., Féraud, G., Bertrand, H., Kampunzu, A.B., Tshoso, G., Watkeys, M.K., Le Gall, B., 2005. Karoo large igneous province: Brevity, origin, and relation to mass extinction questioned by new $^{40}Ar/^{39}Ar$ age data. Geology, 33, 745-748, http://dx.doi.org/10.1130/G21632.1

Juckes, L.M., 1972. The geology of north-eastern Heimefrontfjella, Dronning Maud Land. British Antarctic Survey, Scientific Report, 65, 44 p.

Kawahata, H., Kusakabe, M., Kikuchi, Y., 1987. Strontium, oxygen, and hydrogen isotope geochemistry of hydrothermally altered and weathered rocks in DSDP Hole 504B, Costa Rica Rift. Earth Planet. Sci. Lett., 85, 343-355, http://dx.doi.org/10.1016/0012-821X(87)90132-4

Kent, A.J.R., Baker, J.A., Wiedenbeck, M., 2002. Contamination and melt aggregation processes in continental flood basalts: constraints from melt inclusions in Oligocene basalts from Yemen. Earth Planet. Sci. Lett., 202, 577-594, http://dx.doi.org/10.1016/S0012-821X(02)00823-3

Kogiso, T., Tatsumi, Y., Nakano, S., 1997. Trace element transport during dehydration processes in the subducted oceanic crust: 1. Experiments and implications for the origin of ocean island basalts. Earth Planet. Sci. Lett., 148, 193-205, http://dx.doi.org/10.1016/S0012-821X(97)00018-6

Kreissig, K., Naegler, T.F., Kramers, J.D., van Reenen, D.D., Smit, C.A., 2000. An isotopic and geochemical study of the northern Kaapvaal Craton and the Southern Marginal Zone of the Limpopo Belt: are they juxtaposed terranes? Lithos, 50, 1-25, http://dx.doi.org/10.1016/S0024-4937(99)00037-7

Krynauw, J.R., Hunter, D.R., Wilson, A.H., 1988. Emplacement of sills into wet sediments at Grunehogna, western Dronning Maud Land, Antarctica. J. Geol. Soc. London, 145, 1019-1032, http://dx.doi.org/10.1144/gsjgs.145.6.1019

Krynauw, J.R., Watters, B.R., Hunter, D.R., Wilson, A.H., 1991. A review of the field relations, petrology and geochemistry of the Borgmassivet intrusions in the Grunehogna Province, western Dronning Maud Land, Antarctica. In: Thomson, M.R.A., Crame, J.A., Thomson, J.W. (Eds.), Geological evolution of Antarctica; proceedings of the Fifth international symposium on Antarctic earth sciences, Cambridge University Press, Cambridge, pp. 33-39

le Roex, A.P., Dick, H.J.B., Erlank, A.J., Reid, A.M., Frey, F.A., Hart, S.R., 1983. Geochemistry, Mineralogy and Petrogenesis of Lavas Erupted along the Southwest Indian Ridge Between the Bouvet Triple Junction and 11 Degrees East. J. Petrol., 24, 267-318, http://dx.doi.org/10.1093/petrology/24.3.267

le Roex, A.P., Dick, H.J.B., Watkins, R.T., 1992. Petrogenesis of anomalous K-enriched MORB from the Southwest Indian Ridge: 11°53'E to 14°38'E. Contrib. Miner. Petrol., 110, 253-268, http://dx.doi.org/10.1007/BF00310742

Le Roux, V., Lee, C.A., Turner, S.J., 2010. Zn/Fe systematics in mafic and ultramafic systems: implications for detecting major element heterogeneities in the Earth's mantle. Geochim. Cosmochim. Acta, 74, 2779-2796, http://dx.doi.org/10.1016/j.gca.2010.02.004

Leitch, A.M., Davies, G.F., 2001. Mantle plumes and flood basalts: enhanced melting from plume ascent and an eclogite component. J. Geophys. Res. B, 106, 2047-2059, http://dx.doi.org/10.1029/2000JB900307

Li, C., Ripley, E.M., 2010. The relative effects of composition and temperature on olivine-liquid Ni partitioning: Statistical deconvolution and implications for petrologic modeling. Chem. Geol., 275, 99-104, http://dx.doi.org/10.1016/j.chemgeo.2010.05.001

Lightfoot, P.C., Hawkesworth, C.J., Hergt, J.M., Naldrett, A.J., Gorbachev, N.S., Fedorenko, V.A., Doherty, W., 1993. Remobilisation of the continental lithosphere by a mantle plume: major-, trace-element, and Sr-, Nd-, and Pb-isotope evidence from picritic and tholeiitic lavas of the Noril'sk District, Siberian Trap, Russia. Contrib. Mineral. Petrol., 114, 171-188, http://dx.doi.org/10.1007/BF00307754

Lightfoot, P.C., Naldrett, A.J., Gorbachev, N.S., Doherty, W., Fedorenko, V.A., 1990. Geochemistry of the Siberian Trap of the Noril'sk area, USSR, with implications for the relative contributions of crust and mantle to flood basalt magmatism. Contrib. Mineral. Petrol., 104, 631-644, http://dx.doi.org/10.1007/BF01167284

Liu, Y., Gao, S., Lee, C.A., Hu, S., Liu, X., Yuan, H., 2005. Melt–peridotite interactions: Links between garnet pyroxenite and high-Mg# signature of continental crust. Earth Planet. Sci. Lett., 234, 39-57, http://dx.doi.org/10.1016/j.epsl.2005.02.034

Luttinen, A.V., Furnes, H., 2000. Flood basalts of Vestfjella: Jurassic magmatism across an Archaean-Proterozoic lithospheric boundary in Dronning Maud Land, Antarctica. J. Petrol., 41, 1271-1305, http://dx.doi.org/10.1093/petrology/41.8.1271

Luttinen, A.V., Leat, P.T., Furnes, H., 2010. Björnnutane and Sembberget basalt lavas and the geochemical provinciality of Karoo magmatism in western Dronning Maud Land, Antarctica. J. Volcanol. Geotherm. Res., 198, 1-18, http://dx.doi.org/10.1016/j.jvolgeores.2010.07.011

Luttinen, A.V., Rämö, O.T., Huhma, H., 1998. Neodymium and strontium isotopic and trace element composition of a Mesozoic CFB suite from Dronning Maud Land, Antarctica: Implications for lithosphere

and asthenosphere contributions to Karoo magmatism. Geochim. Cosmochim. Acta, 62, 2701-2714, http://dx.doi.org/10.1016/S0016-7037(98)00184-7

Mahoney, J.J., le Roex, A.P., Peng, Z., Fisher, R.L., Natland, J.H., 1992. Southwestern limits of Indian Ocean ridge mantle and the origin of low $^{206}Pb/^{204}Pb$ mid-ocean ridge basalt: isotope systematics of the central Southwest Indian Ridge (17°-50°E). J. Geophys. Res., 97, 19771-19790, http://dx.doi.org/10.1029/92JB01424

Mallik, A., Dasgupta, R., 2012. Reaction between MORB-eclogite derived melts and fertile peridotite and generation of ocean island basalts. Earth Planet. Sci. Lett., 329–330, 97-108, http://dx.doi.org/10.1016/j.epsl.2012.02.007

Marschall, H.R., Hawkesworth, C.J., Storey, C.D., Dhuime, B., Leat, P.T., Meyer, H.-., Tamm-Buckle, S., 2010. The Annandagstoppane Granite, East Antarctica: Evidence for Archaean Intracrustal recycling in the Kaapvaal-Grunehogna Craton from zircon O and Hf isotopes. J. Petrol., 51, 2277-2301, http://dx.doi.org/10.1093/petrology/egq057

Molzahn, M., Reisberg, L., Wörner, G., 1996. Os, Sr, Nd, Pb, O isotope and trace element data from the Ferrar flood basalts, Antarctica: evidence for an enriched subcontinental lithospheric source. Earth Planet. Sci. Lett., 144, 529-545, http://dx.doi.org/10.1016/S0012-821X(96)00178-1

Moyes, A.B., Krynauw, J.R., Barton, J.M.,Jr, 1995. The age of the Ritscherflya Supergroup and Borgmassivet Intrusions, Dronning Maud Land, Antarctica. Antarct. Sci., 7, 87-97, http://dx.doi.org/10.1017/S0954102095000125

Murphy, J.B., Dostal, J., Nance, R.D., Keppie, J.D., 2004. Neoproterozoic juvenile crust development in the peri-Rodinian ocean: Implications for Grenvillian orogenesis. Geol. Soc. Am. Mem., 197, 135-144, http://dx.doi.org/10.1130/0-8137-1197-5.135

Obata, M., Nagahara, N., 1987. Layering of alpine-Type peridotite and the segregation of partial melt in the upper mantle. J. Geophys. Res. B, 92, 3467-3474, http://dx.doi.org/10.1029/JB092iB05p03467

Pik, R., Deniel, C., Coulon, C., Yirgu, G., Marty, B., 1999. Isotopic and trace element signatures of Ethiopian flood basalts: evidence for plume-lithosphere interactions. Geochim. Cosmochim. Acta, 63, 2263-2279, http://dx.doi.org/10.1016/S0016-7037(99)00141-6

Plank, T., Langmuir, C.H., 1998. The chemical composition of subducting sediment and its consequences for the crust and mantle. Chem. Geol., 145, 325-394, http://dx.doi.org/10.1016/S0009-2541(97)00150-2

Prytulak, J., Elliott, T., 2007. TiO_2 enrichment in ocean island basalts. Earth Planet. Sci. Lett., 263, 388-403, http://dx.doi.org/10.1016/j.epsl.2007.09.015

Richards, M.A., Duncan, R.A., Courtillot, V.E., 1989. Flood basalts and hot-spot tracks: plume heads and tails. Science, 246, 103-107, http://dx.doi.org/10.1126/science.246.4926.103

Riley, T.R., Leat, P.T., Curtis, M.L., Millar, I.L., Duncan, R.A., Fazel, A., 2005. Early-Middle Jurassic dolerite dykes from Western Dronning Maud Land (Antarctica): Identifying mantle sources in the Karoo Large Igneous Province. J. Petrol., 46, 1489-1524, http://dx.doi.org/10.1093/petrology/egi023

Riley, T.R., Millar, I.L. Geochemistry of the 1100Ma intrusive rocks from the Ahlmannryggen region, Dronning Maud Land, Antarctica. Antarct. Sci., in press, http://dx.doi.org/10.1017/S0954102013000916

Rocha-Júnior, E.R.V., Puchtel, I.S., Marques, L.S., Walker, R.J., Machado, F.B., Nardy, A.J.R., Babinski, M., Figueiredo, A.M.G., 2012. Re–Os isotope and highly siderophile element systematics of the Paraná continental flood basalts (Brazil). Earth Planet. Sci. Lett., 337-338, 164-173, http://dx.doi.org/10.1016/j.epsl.2012.04.050

Rudnick, R.L., Barth, M., Horn, I., McDonough, W.F., 2000. Rutile-Bearing Refractory Eclogites: Missing Link Between Continents and Depleted Mantle. Science, 287, 278-281, http://dx.doi.org/10.1126/science.287.5451.278

Sakuyama, T., Tian, W., Kimura, J., Fukao, Y., Hirahara, Y., Takahashi, T., Senda, R., Chang, Q., Miyazaki, T., Obayashi, M., Kawabata, H., Tatsumi, Y., 2013. Melting of dehydrated oceanic crust from the stagnant slab and of the hydrated mantle transition zone: Constraints from Cenozoic alkaline basalts in eastern China. Chem. Geol., 359, 32-48, http://dx.doi.org/10.1016/j.chemgeo.2013.09.012

Sano, T., Fujii, T., Deshmukh, S.S., Fukuoka, T., Aramaki, S., 2001. Differentiation processes of Deccan Trap basalts: contribution from geochemistry and experimental petrology. J. Petrol., 42, 2175-2195, http://dx.doi.org/10.1093/petrology/42.12.2175

Shirey, S.B., 1997. Re-Os isotopic compositions of Midcontinent rift system picrites: implications for plume – lithosphere interaction and enriched mantle sources. Can. J. Earth Sci., 34, 489-503, http://dx.doi.org/10.1139/e17-040

Shirey, S.B., Walker, R.J., 1998. The Re-Os isotope system in cosmochemistry and high-temperature geochemistry. Annu. Rev. Earth Planet. Sci., 26, 423-500, http://dx.doi.org/10.1146/annurev.earth.26.1.423

Simon, N.S., Carlson, R.W., Graham Pearson, D., Davies, G.R., 2007. The origin and evolution of the Kaapvaal cratonic lithospheric mantle. J. Petrol., 48, 589-625, http://dx.doi.org/10.1093/petrology/egl074

Sobolev, A.V., Hofmann, A.W., Brügmann, G., Batanova, V.G., Kuzmin, D.V., 2008. A quantitative link between recycling and osmium isotopes. Science, 321, 536, http://dx.doi.org/10.1126/science.1158452

Sobolev, A.V., Hofmann, A.W., Jochum, K.P., Kuzmin, D.V., Stoll, B., 2011a. A young source for the Hawaiian plume. Nature, 476, 434-437, http://dx.doi.org/10.1038/nature10321

Sobolev, A.V., Hofmann, A.W., Jochum, K.P., Kuzmin, D.V., Stoll, B., 2011b. Linking mantle plumes, large igneous provinces and environmental catastrophes. Nature, 477, 312-316, http://dx.doi.org/10.1038/nature10385

Sobolev, A.V., Hofmann, A.W., Kuzmin, D.V., Yaxley, G.M., Arndt, N.T., Chung, S., Danyushevsky, L.V., Elliott, T., Frey, F.A., Garcia, M.O., Gurenko, A.A., Kamenetsky, V.S., Kerr, A.C., Krivolutskaya, N.A., Matvienkov, V.V., Nikogosian, I.K., Rocholl, A., Sigurdsson, I.A., Sushchevskaya, N.M., Teklay, M., 2007. The amount of recycled crust in sources of mantle-derived melts. Science, 316, 412-417, http://dx.doi.org/10.1126/science.113811

Spera, F.J., Bohrson, W.A., 2001. Energy-constrained open-system magmatic processes I: General model and energy-constrained assimilation and fractional crystallization (EC-AFC) formulation. J. Petrol., 42, 999-1018, http://dx.doi.org/10.1093/petrology/42.5.999

Storey, M., Mahoney, J.J., Saunders, A.D., 1997. Cretaceous basalts in Madagascar and the transition between plume and continental lithosphere mantle sources. In: Mahoney, J.J., Coffin, M.F. (Eds.), Large igneous provinces: continental, oceanic, and planetary flood volcanism. Geophysical Monograph, 100. American Geophysical Union, United States, pp. 95-122, http://dx.doi.org/10.1029/GM100p0095

Stracke, A., Bizimis, M., Salters, V.J.M., 2003. Recycling oceanic crust: quantitative constraints. Geochem. Geophys. Geosyst., 4, http://dx.doi.org/10.1029/2001GC000223

Sun, S.S., McDonough, W.F., 1989. Chemical and isotopic systematics of oceanic basalts: Implications for mantle composition and processes. In: Saunders, A.D., Norry, M.J. (Eds.), Magmatism in the ocean basins. Geological Society Special Publications, 42, United Kingdom (GBR), pp. 313-345, http://dx.doi.org/10.1144/GSL.SP.1989.042.01.19

Sweeney, R.J., Duncan, A.R., Erlank, A.J., 1994. Geochemistry and petrogenesis of central Lebombo basalts of the Karoo igneous province. J. Petrol., 35, 95-125, http://dx.doi.org/10.1093/petrology/35.1.95

Thompson, R.N., Gibson, S.A., 2000. Transient high temperatures in mantle plume heads inferred from magnesian olivines in Phanerozoic picrites. Nature, 407, 502-506, http://dx.doi.org/10.1038/35035058

Todt, W., Cliff, R.A., Hanser, A., Hofmann, A.W., 1996. Evaluation of a ^{202}Pb-^{205}Pb double spike for high-precision lead isotope analysis. In: Basu, A.R., Hart, S.R. (Eds.), Earth Processes: Reading the Isotopic Code. Geophysical Monograph, 95. American Geophysical Union, United States, pp. 429-437.

Tuff, J., Takahashi, E., Gibson, S.A., 2005. Experimental constraints on the role of garnet pyroxenite in the genesis of high-Fe mantle plume derived melts. J. Petrol., 46, 2023-2058, http://dx.doi.org/10.1093/petrology/egi046

Walker, R.J., Carlson, R.W., Shirey, S.B., Boyd, F.R., 1989. Os, Sr, Nd, and Pb isotope systematics of Southern African peridotite xenoliths: Implications for the chemical evolution of subcontinental mantle. Geochim. Cosmochim. Acta, 53, 1583-1595, http://dx.doi.org/10.1016/0016-7037(89)90240-8

Wareham, C.D., Pankhurst, R.J., Thomas, R.J., Storey, B.C., Grantham, G.H., Jacobs, J., Eglington, B.M., 1998. Pb, Nd, and Sr Isotope Mapping of Grenville-Age Crustal Provinces in Rodinia. J. Geol., 106, 647-660, http://dx.doi.org/10.1086/516051

Wolmarans, L.C., Kent, K.E., 1982. Geological investigations in western Dronning Maud Land, Antarctica - a synthesis. S. Afr. J. Antarc. Res., Suppl., 2, 93 p.

Woodhead, J.D., Devey, C.W., 1993. Geochemistry of the Pitcairn seamounts I: Source character and temporal trends. Earth Planet. Sci. Lett., 116, 81-99, http://dx.doi.org/10.1016/0012-821X(93)90046-C

Workman, R.K. and Hart, S.R., 2005. Major and trace element composition of the depleted MORB mantle (DMM). Earth Planet. Sci. Lett., 231, 53-72, http://dx.doi.org/10.1016/j.epsl.2004.12.005

Workman, R.K., Hart, S.R., Jackson, M.G., Regelous, M., Farley, K.A., Blusztajn, J.S., Kurz, M., Staudigel, H., 2004. Recycled metasomatized lithosphere as the origin of the enriched mantle II (EM2) end-member: Evidence from the Samoan volcanic chain. Geochem. Geophys. Geosyst., 5, http://dx.doi.org/10.1029/2003GC000623

Yaxley, G.M., Green, D.H., 1998. Reactions between eclogite and peridotite; mantle refertilisation by subduction of oceanic crust; IEC 97; Fifth international eclogite conference. Schweiz. Miner. Petrog., 78, 243-255

Zindler, A., Hart, S.R., 1986. Chemical geodynamics. Annu. Rev. Earth Planet. Sci., 14, 493-571, http://dx.doi.org/10.1146/annurev.ea.14.050186.002425

Figure captions

Fig. 1. Outcrop map of western Dronning Maud Land from Vestfjella to H. U. Svedrupfjella. Distribution of Karoo flood basalts and Ahlmannryggen Group 3 dikes shown. Lithospheric boundary between Grunehogna craton and Maud belt is after Corner (1994). Distribution of Karoo flood basalts and related intrusive rocks (outside the flood basalt areas) in reconstructed Gondwana supercontinent (cf. Heinonen et al., 2010) is shown in the inset.

Fig. 2. Sr and Nd isotopic characteristics of the Ahlmannryggen Group 3dikes (Riley et al., 2005) shown at 180 Ma. Data for Vestfjella depleted (D-FP) and enriched (E-FP) ferropicrite suites (Heinonen and Luttinen, 2008; Heinonen et al., 2010), Karoo CFBs (Ellam and Cox, 1989, 1991; Harris et al., 1990; Hawkesworth et al., 1984; Jourdan et al., 2007; Luttinen and Furnes, 2000; Luttinen et al., 1998, 2010; Riley et al., 2005; Sweeney et al., 1994), SWIR MORB (le Roex et al., 1983, 1992; Mahoney et al., 1992), and depleted MORB mantle (DMM; Workman and Hart, 2005) also presented. The isotopic compositions of SWIR MORB sources and DMM were back-calculated using DMM isotopic ratios after Workman and Hart (2005). Lithospheric contamination models after Heinonen et al. (2010).

Fig. 3. $^{87}Sr/^{86}Sr$ vs. $^{206}Pb/^{204}Pb$ (a), ε_{Nd} vs. $^{206}Pb/^{204}Pb$ (b), $^{207}Pb/^{204}Pb$ vs. $^{206}Pb/^{204}Pb$ (c), and $^{208}Pb/^{204}Pb$ vs. $^{206}Pb/^{204}Pb$ (d) compositions of the Ahlmannryggen Group 3 dikes in comparison with Karoo CFBs (Ellam and Cox, 1989, 1991; Jourdan et al., 2007), Vestfjella depleted and enriched ferropicrite suites (Heinonen an Luttinen, 2008; Heinonen et al., 2010), SWIR MORB (le Roex et al., 1983, 1992; Mahoney et al., 1992), depleted MORB mantle (DMM; Workman and Hart, 2005), prevalent mantle component (PREMA, $^{208}Pb/^{204}Pb$ not defined; Zindler and Hart, 1986) and non-chondritic primitive mantle (NCPM; cf. Jackson and Carlson, 2011; Jackson and Jellinek, 2013; Pb isotope composition constrained by 4.50 Ga and 4.43 Ga isochrons) at 180 Ma. The compositions of SWIR MORB sources and DMM were back-calculated using DMM isotopic ratios after Workman and Hart (2005) and the Sr and Nd composition of NCPM was back-calculated following Jackson and Jellinek (2013). PREMA at 180 Ma was approximated using E-DMM isotopic ratios after Workman and Hart (2005).

Fig. 4. ε_{Nd} vs. $^{187}Os/^{188}Os$ compositions of the Ahlmannryggen Group 3 dikes in comparison with the Vestfjella depleted and enriched ferropicrites suites (Heinonen and Luttinen, 2008; Heinonen et al., 2010), Mwenezi picrites (Ellam and Cox, 1989; Ellam et al., 1992), OIBs that sample enriched mantle (EM) domains (Eisele et al., 2002; Woodhead and Devey, 1993; Workman et al., 2004), Gondwana SCLM (estimated after mantle xenoliths; Simon et al., 2007; Walker et al., 1989), and depleted MORB mantle (DMM; Shirey and Walker, 1998; Workman and Hart, 2005) at 180 Ma. In the case of mantle reservoirs, the isotopic compositions were back-calculated using $^{187}Re/^{188}Os$ of 1.6 (DMM) and 0.4 (EM) (cf. Shirey and Walker, 1998) and $^{147}Sm/^{144}Nd$ of 0.2485 (DMM; after Workman and Hart, 2005), 0.2138 (EM1; after Eisele et al., 2002), and 0.1840 (EM2; after Workman et al., 2004). EC-AFC models for a Group 3 high-ε_{Nd} parental magma with high-Os and low-Os upper (Archean) crustal contaminants (UC) also illustrated (see Table S2 for parameters).

Fig. 5. $^{87}Sr/^{86}Sr$ vs. $^{206}Pb/^{204}Pb$ (a), ε_{Nd} vs. $^{206}Pb/^{204}Pb$ (b), $^{207}Pb/^{204}Pb$ vs. $^{206}Pb/^{204}Pb$ (c), and $^{208}Pb/^{204}Pb$ vs. $^{206}Pb/^{204}Pb$ (d) compositions of the Ahlmannryggen Group 3 dikes at 180 Ma in comparison with EC-AFC models (Table S2) involving a Group 3 high-ε_{Nd} parental magma and various Archean (TTGs, amphibolites, and metasedimentary rocks from the Kaapvaal Craton; models marked in gray) and Proterozoic (Ritscherflya metasedimentary rock, Sverdupfjella gneiss, and Borgmassivet mafic intrusion; models marked in black) crustal contaminants (see Table S2 for detailed model parameters and references). Tick marks indicating 1–10 % of assimilation with one-percent intervals shown for Archean TTG 96/228 and Proterozoic contaminants; the degree of contamination is similar also in the case of other Archean contamination trends, tick marks have not been marked to preserve clarity. Compositions of Karoo CFBs, Vestfjella

depleted and enriched ferropicrite suites, SW Indian Ridge MORBs, and depleted MORB mantle (DMM) also shown at 180 Ma (cf. Fig. 3).

Fig. 6. Primitive mantle –normalized (Sun and McDonough, 1989) incompatible trace element diagrams of the uncontaminated (ε_{Nd} = +9) Group 3 dikes. Average MORB (Gale et al., 2013), variably subduction-modified MORB (1 with 100% modification, 2 with 50% modification; Kogiso et al., 1997; cf. section 5.2.2.), mixture (9:1) of DMM (Workman and Hart, 2005) and sm-MORB 2, simple modal partial melt model of the mixture (details given in Table S3), and average Ronda Group C websterite (Bodinier et al., 2008) also shown.

Fig. 7. $^{87}Sr/^{86}Sr$ vs. $^{206}Pb/^{204}Pb$ (a), ε_{Nd} vs. $^{206}Pb/^{204}Pb$ (b), $^{207}Pb/^{204}Pb$ vs. $^{206}Pb/^{204}Pb$ (c), and $^{208}Pb/^{204}Pb$ vs. $^{206}Pb/^{204}Pb$ (d) compositions of the Ahlmannryggen Group 3 dikes with the results of isotopic modeling of recycled subduction-modified MORB (cf. Fig. 6) at 180 Ma. *Black lines* illustrate binary mixing curves between DMM and 0.7 Ga and 1.0 Ga sm-MORB 2 (cf. Fig. 6) with an effect of 30% of seawater alteration (sw) shown in Fig. 7a (seawater alteration has negligible effect on other isotope ratios); square dots indicate 10% and 20% of recycled material in the mixture (only shown for 1.0 Ga curve for clarity). *Gray unbroken line* illustrates binary mixing curve between DMM and 0.7 Ga seawater-altered (30% of Sr replaced) sm-MORB 1 (cf. Fig. 6); square dots indicate 2% and 5% of recycled material in the mixture. *Gray stippled lines* illustrate the composition of 1 Ga recycled unmodified MORB with an additional sedimentary component (sed; Plank and Langmuir, 1998; cf. Stracke et al., 2003) and its mixing with DMM. See Table S4 for detailed model parameters and references. The compositions of the Vestfjella depleted and enriched ferropicrite suites, Karoo CFBs, non-chondritic primitive mantle (NCPM) and PREMA as in Fig. 3.

Fig. 8. $^{206}Pb/^{204}Pb$ vs. $^{187}Os/^{188}Os$ compositions of the uncontaminated (ε_{Nd} = +9) Group 3 dikes and hypothetical mixtures between depleted MORB mantle peridotite (DMM) and 0.7 Ga sm-MORB 2 (cf. Fig. 6 and 7). A and B models with Os-rich peridotite and Re-poor MORB (A with 30% loss of Re) and C and D models with Os-poor peridotite and Re-rich MORB (C with 30% loss of Re). See Table S4 for more detailed parameters. Pb isotopic modeling performed as in Fig. 7 (Table S4). It is important to note that due to the low Os content of the recycled MORB, the models involving Os-rich peridotite (A and C) are not notably different whether Re has been subduction-modified or not.

Fig. 9. Primitive mantle –normalized (Sun and McDonough, 1989) garnet-peridotite incompatible trace element diagram for the average uncontaminated Group 3 high-ε_{Nd} dike (cf. Fig. 6), DMM (Workman and Hart, 2005), non-chondritic primitive mantle (NCPM; Jackson and Jellinek, 2013), peridotite component mixtures with sm-MORB 2 (cf. Fig. 6), and partial melts of the mixtures (details given in Table S3).

***Highlights (for review)**

Continental flood basalt –related dikes derive from sublithospheric mantle source

The mantle source was composed of mixture of recycled crust and peridotite

The recycled component was subduction-modified MORB

The peridotite component was DMM, oceanic lithosphere or non-chondritic primitive mantle

Figure 1 (2 columns)
Click here to do"""""loaj high resolution image

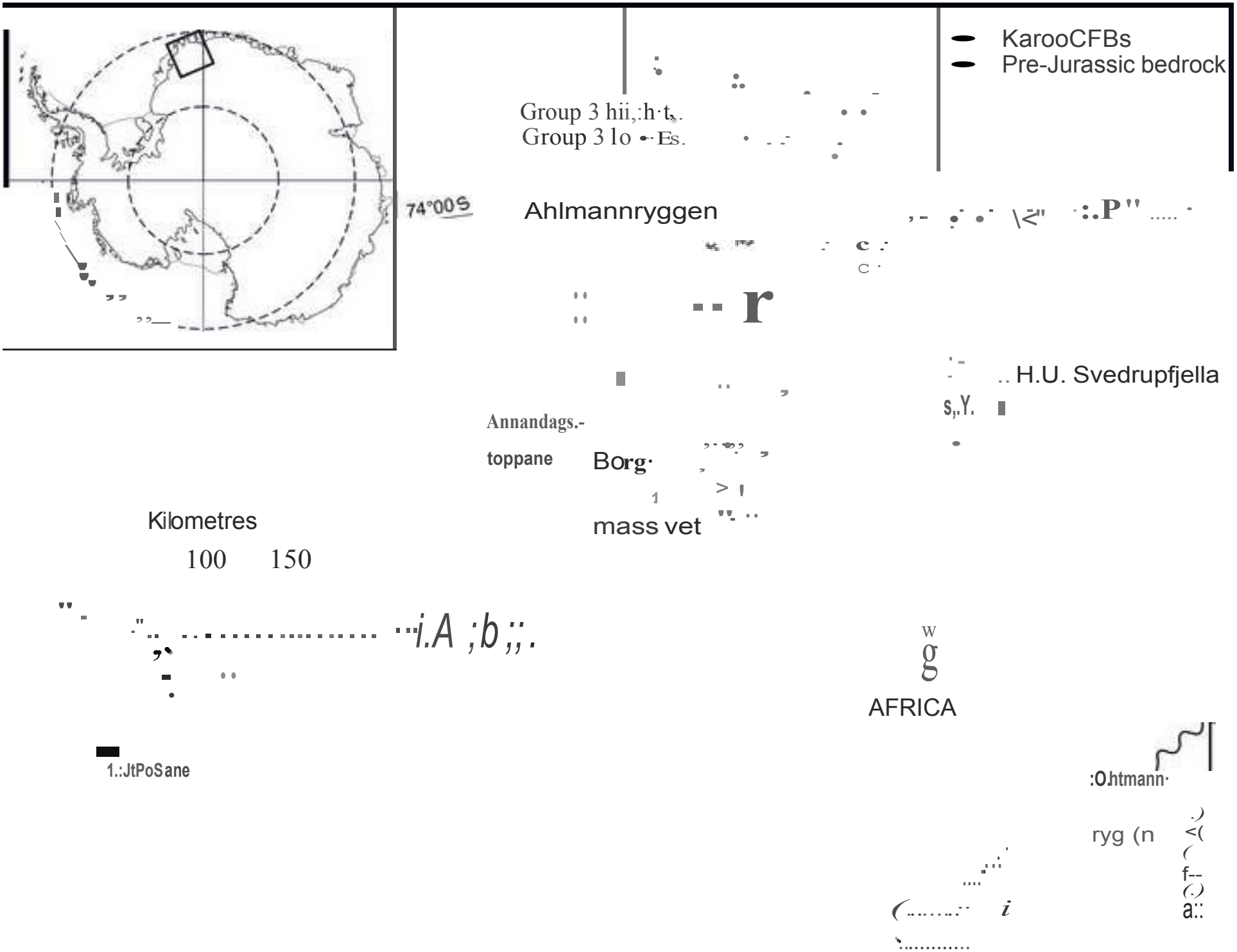

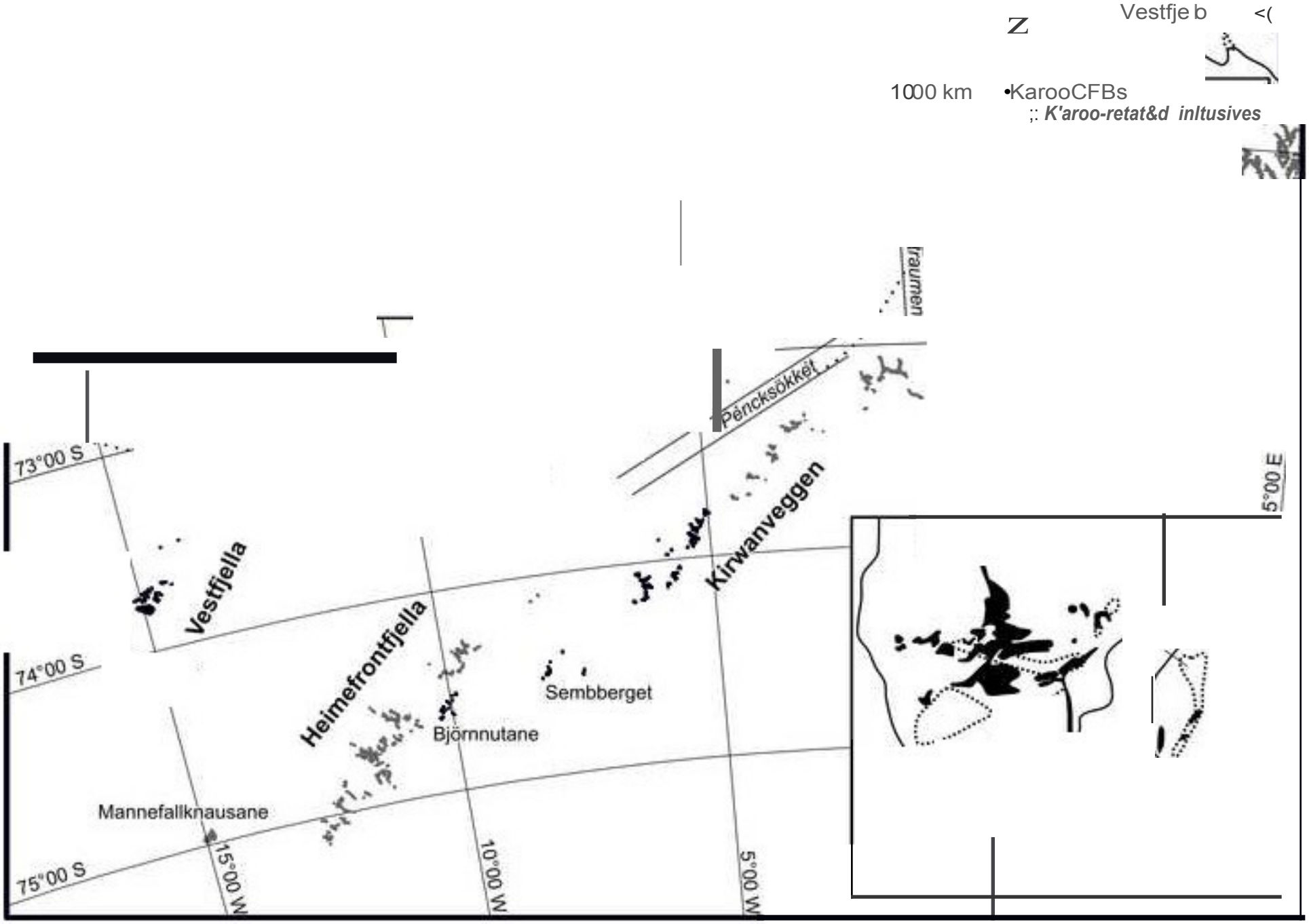
Vestfje b
<(
Z
1000 km
•KarooCFBs
;: K'aroo-retat&d inltusives
Fraumen
Pencksökket
73°00 S
74°00 S
75°00 S
15°00 W
10°00 W
5°00 W
5°00 E
Vestfjella
Heimefrontfjella
Kirwanveggen
Sembberget
Björnnutane
Mannefallknausane

Figure2 (1column)
Click here to do"""""loaj high resolution image

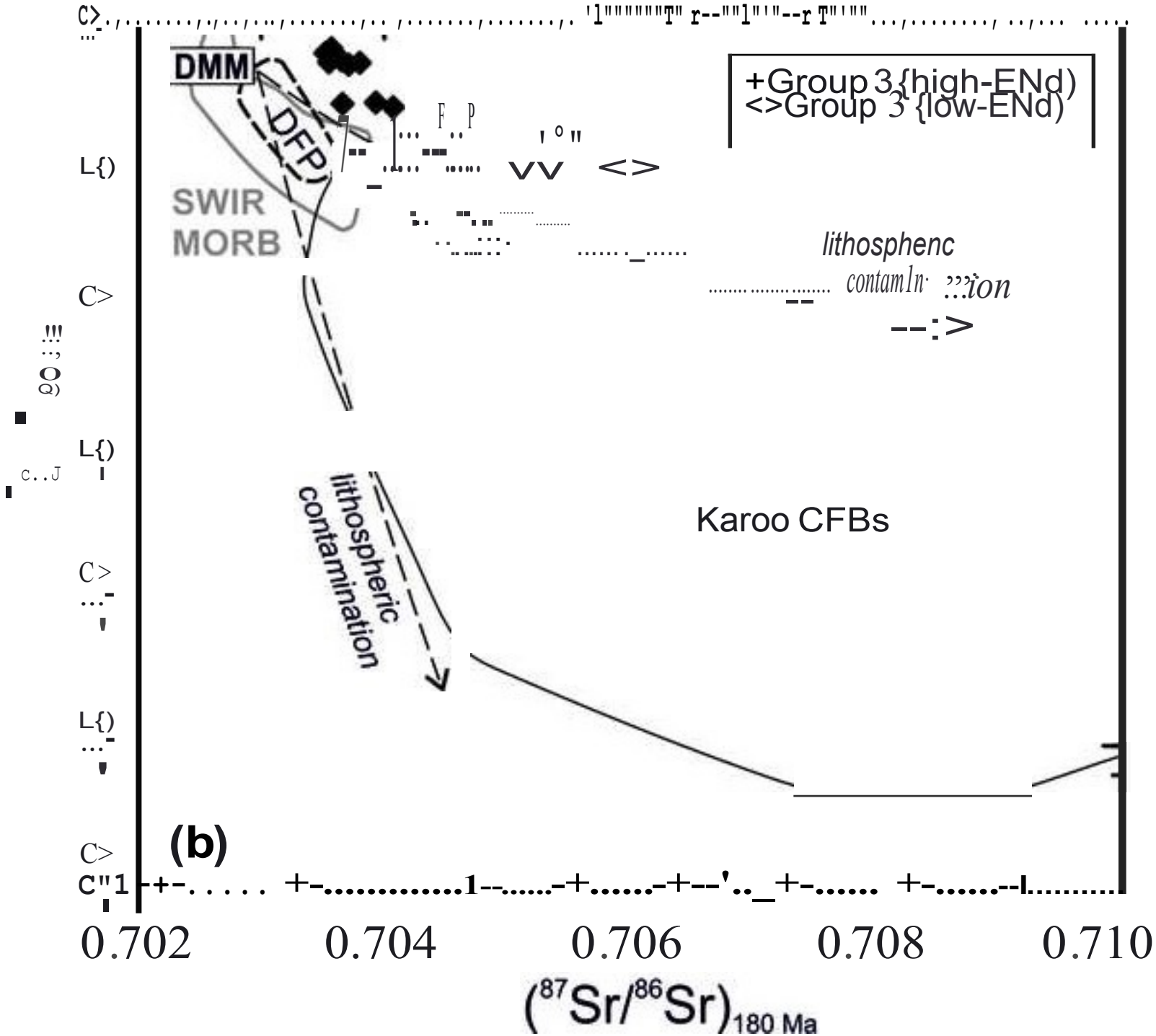

Figure 3 (2 columns)
Click here to do"""loaj high resolution image

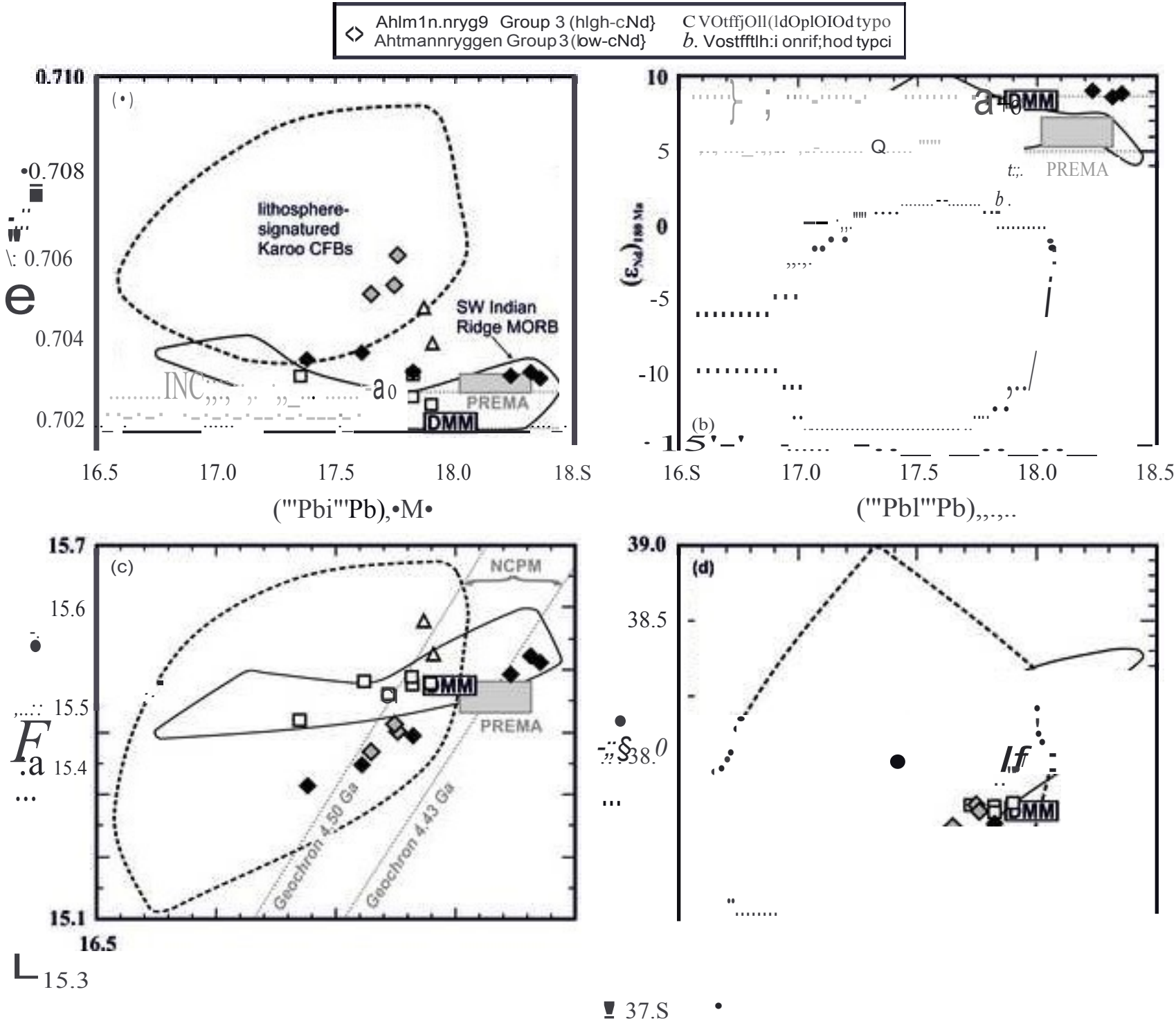

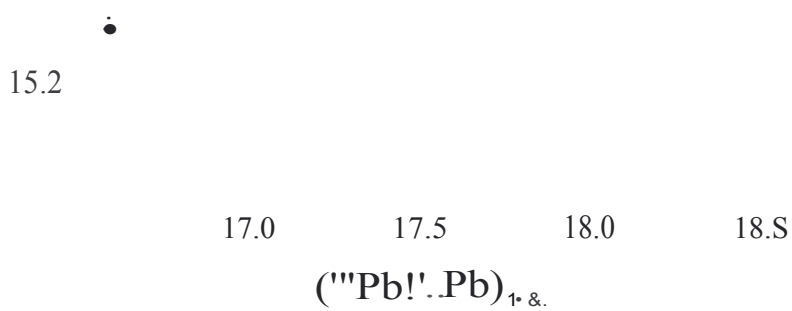
15.2
17.0
17.5
18.0
18.S
('"Pb!'..Pb)1. &.

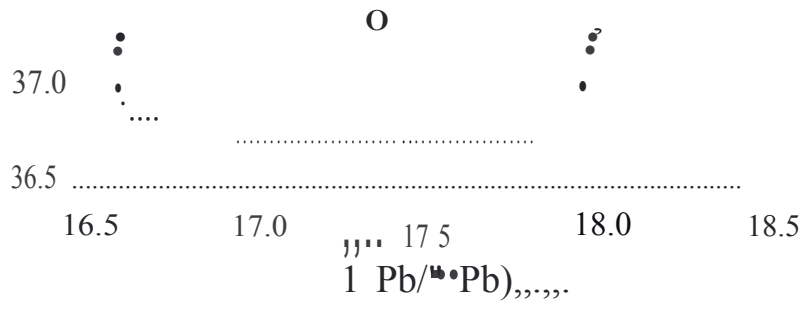
O
37.0
36.5
16.5
17.0
17 5
18.0
18.5
1 Pb/"•Pb),,.,,.

Figure4 (1column)
Click here to do"""loaj high resolution image

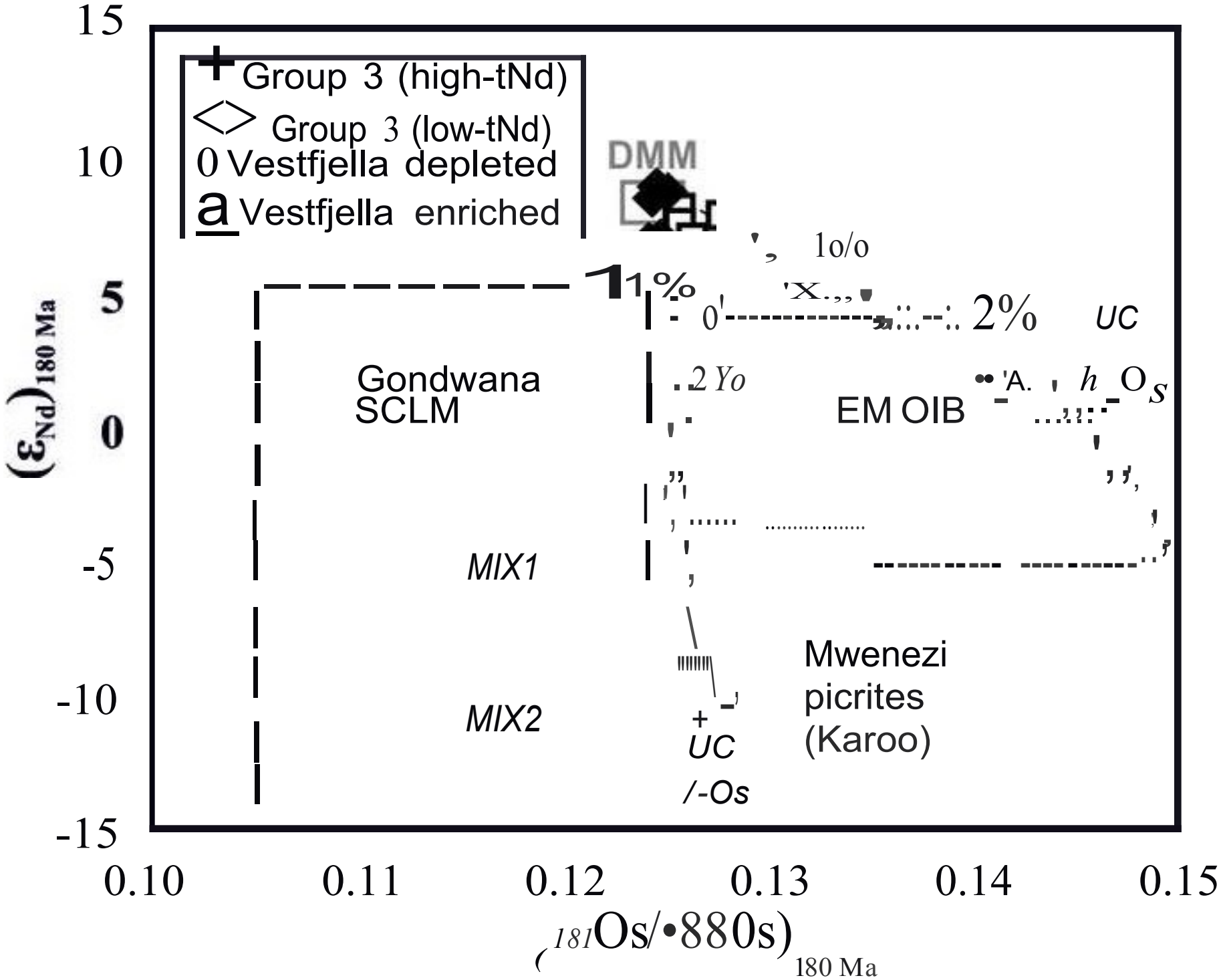

Figure 5 (2 columns)

Click here to do""""loaj high resolution image

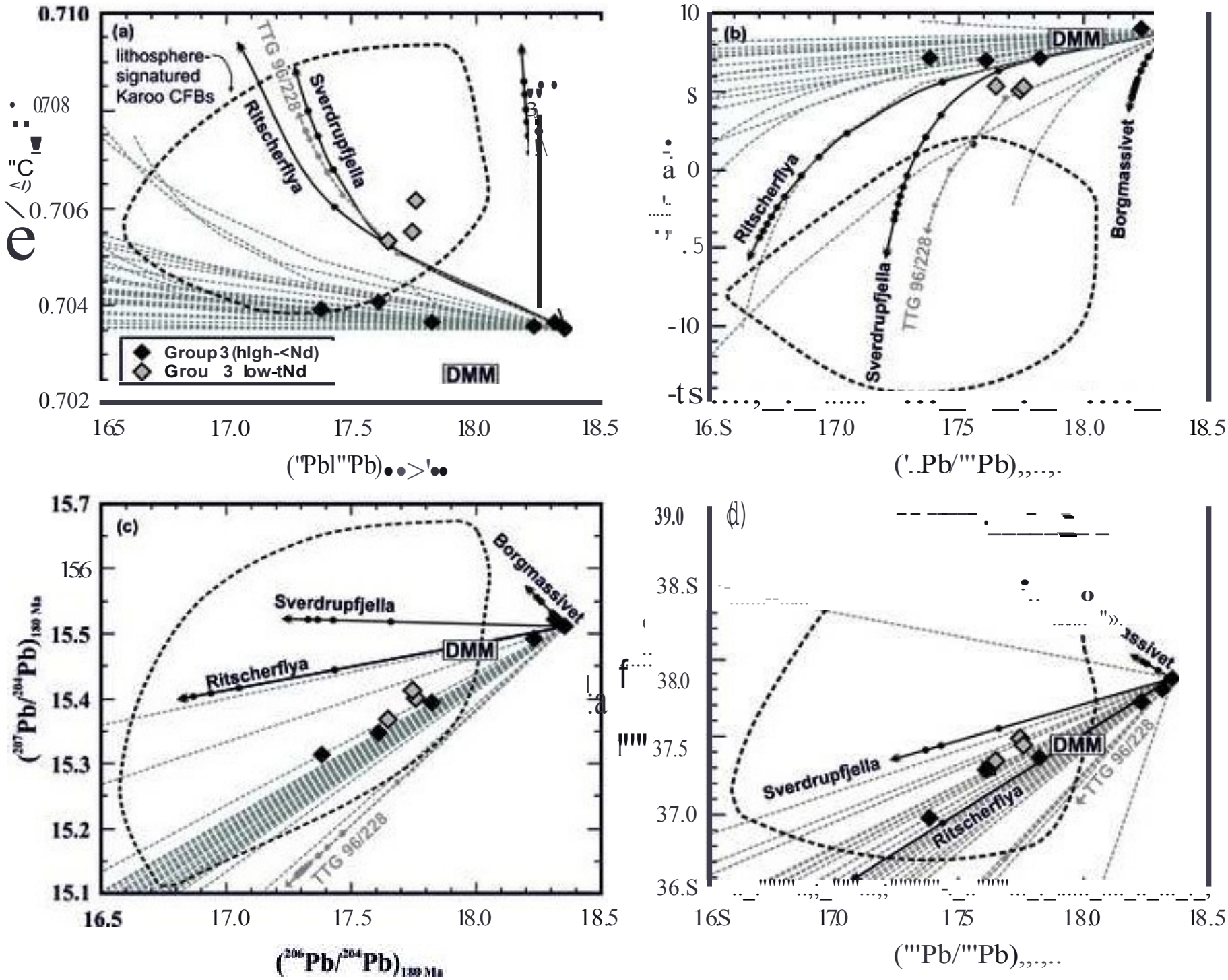

Figures (1.5 columns)
Click here to do"""loaj high resolution image

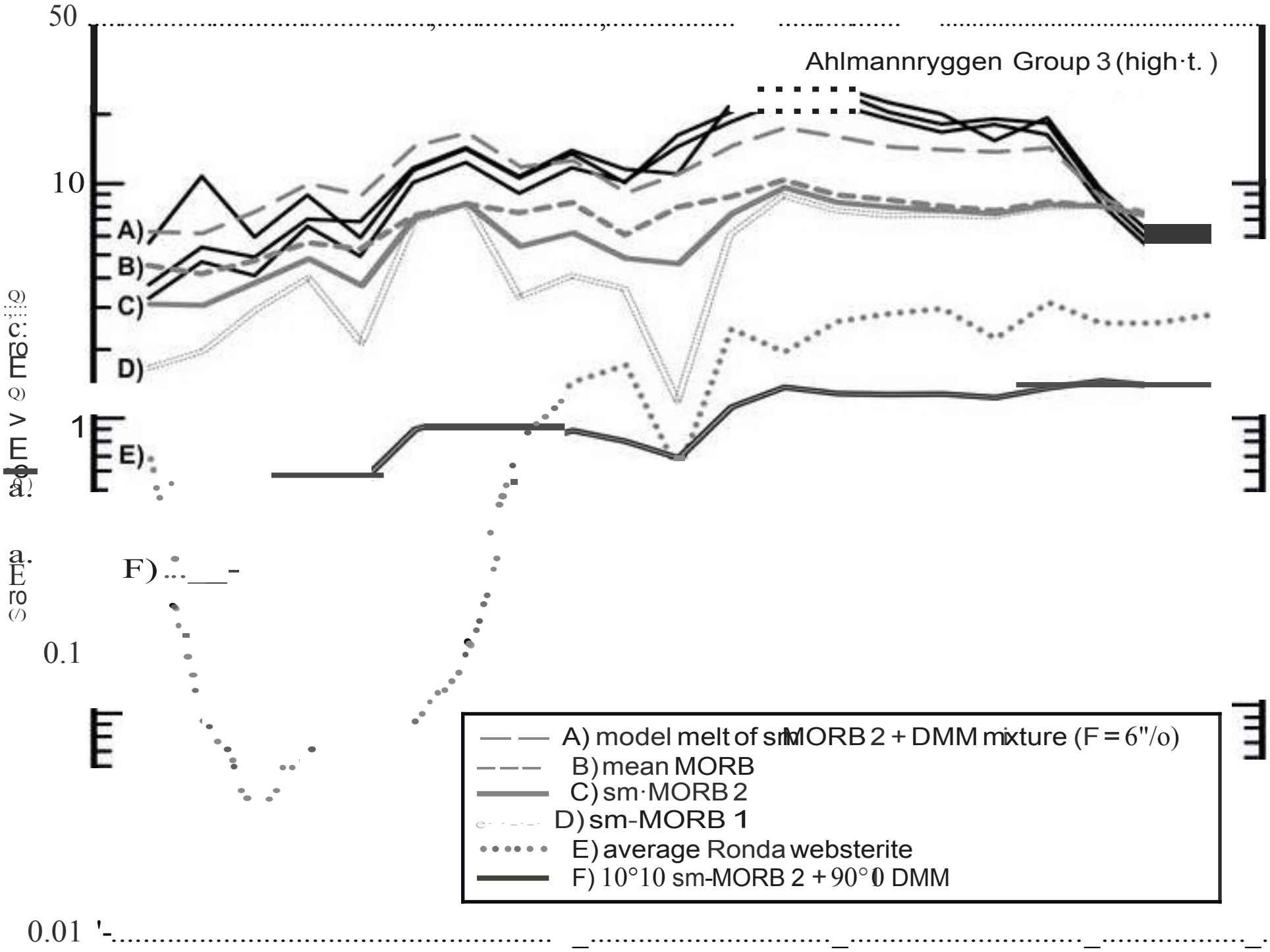

Rb Ba Th U K Nb Ta La Ce Sr Pb Nd Zr Hf Sm Eu Ti Gd Y Yb Lu

Figure 7 (2 columns)
Click here to do"""loaj high resolution image

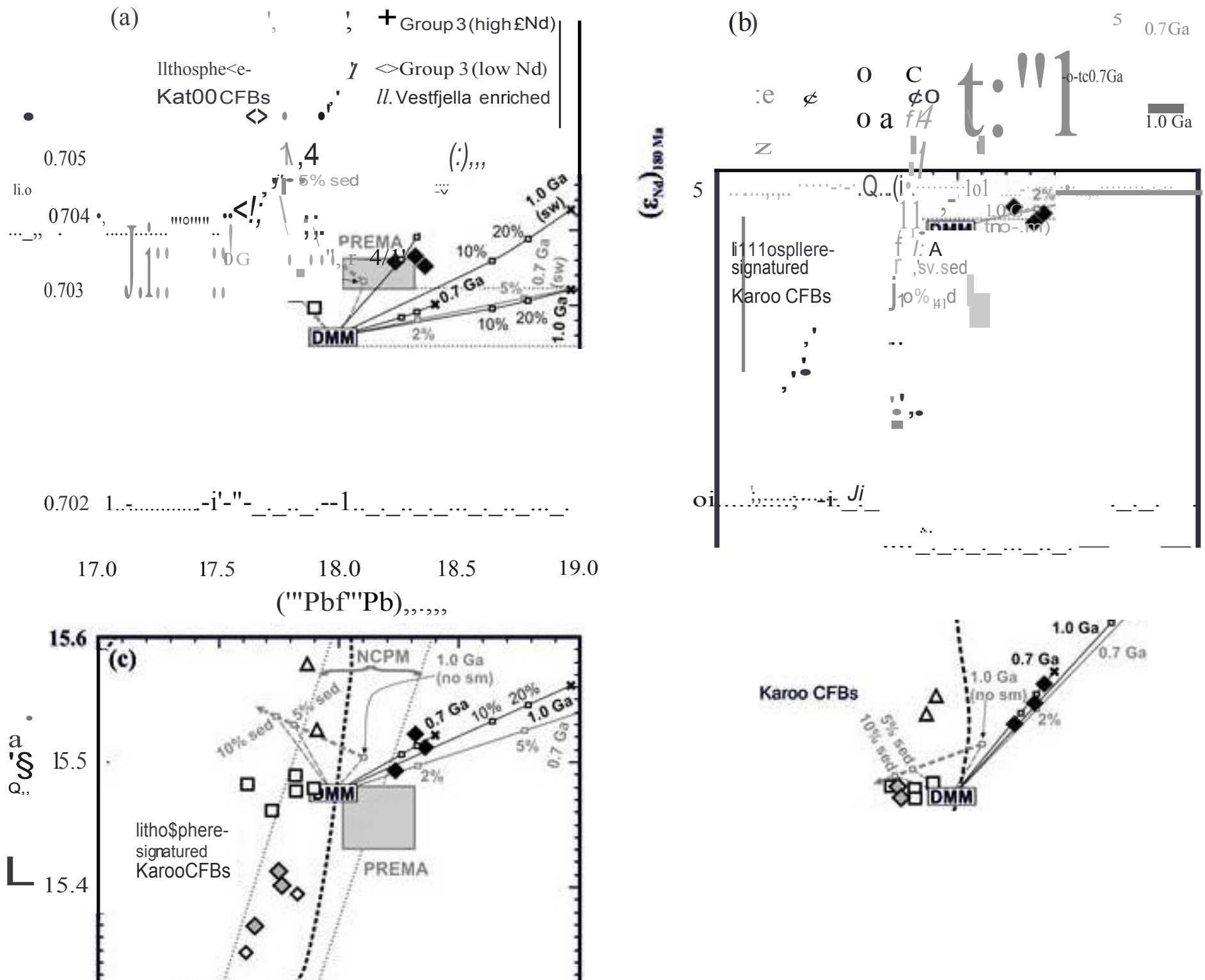

17.5 18.0 18.5 19.0

$(^{206}Pb/^{204}Pb)_{180\ Ma}$

Figures (1column)
Click here to do"""loaj high resolution image

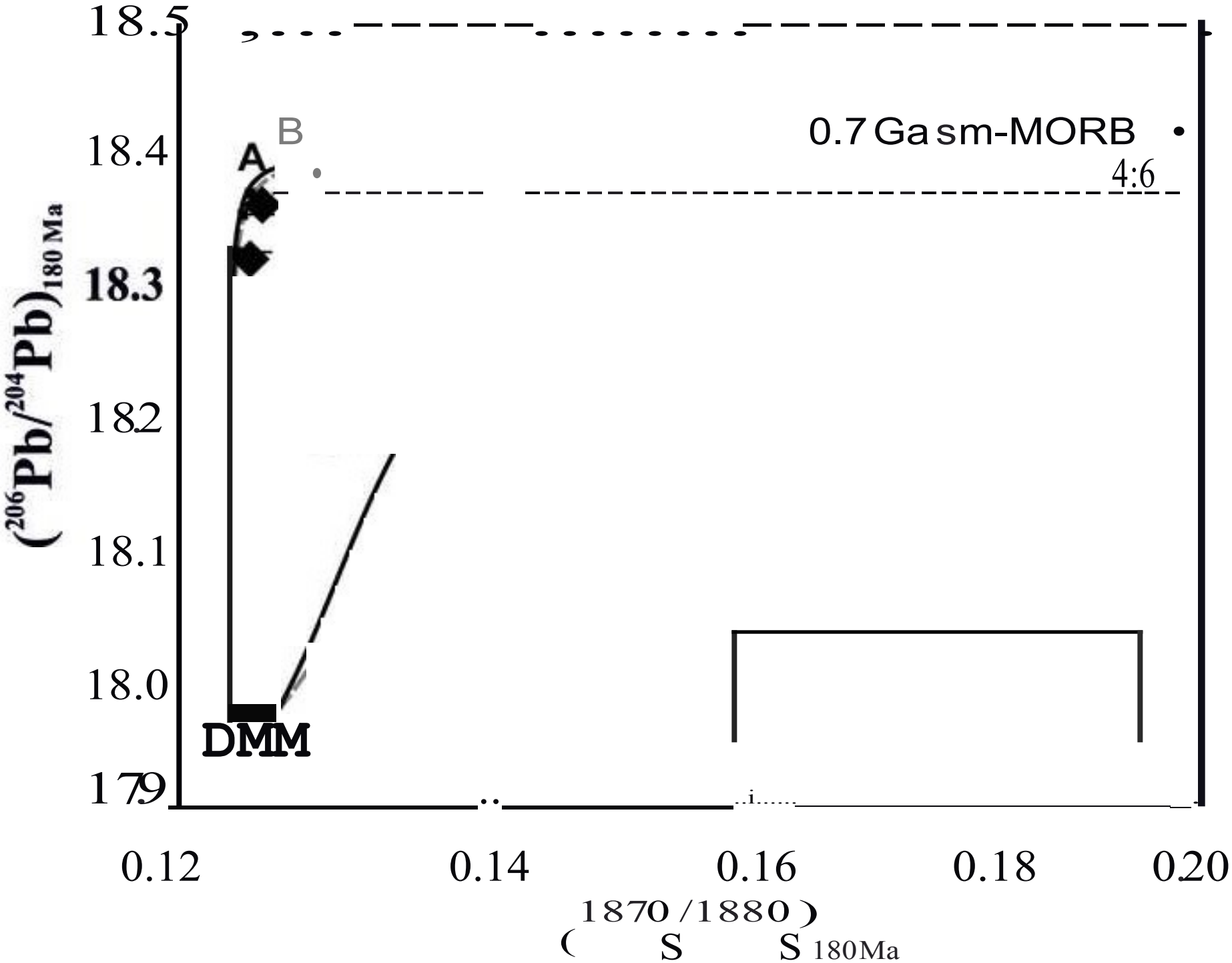

Figures (1.5 columns)
Click here to do"""loaj high resolution image

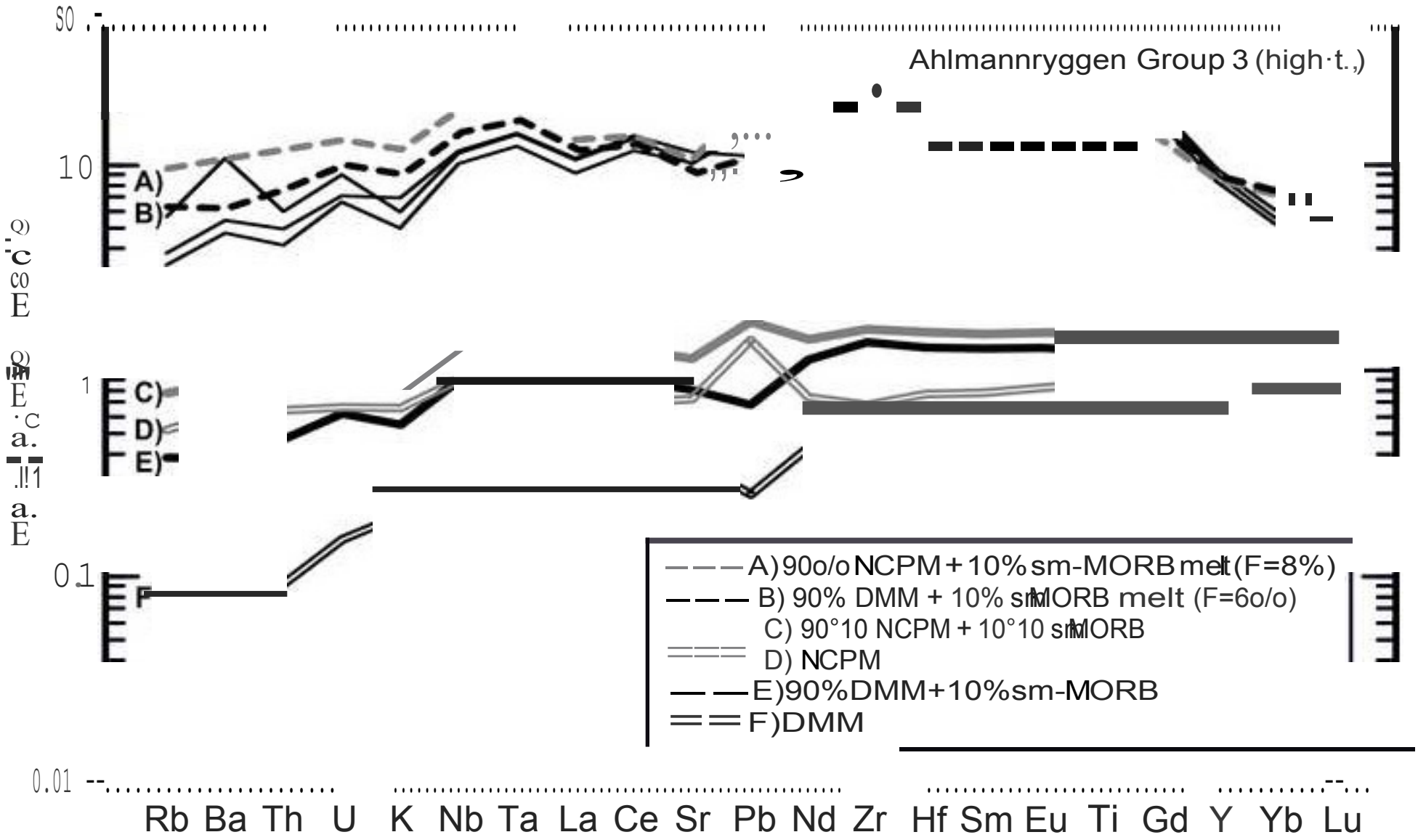

Table 1
Click here to download Table: Table1.docx

Table 1

Whole-rock major element (normalized to 100% volatile free) and Sr, Nd, Pb, and Os isotopic composition of Group 3 samples from Ahlmannryggen (western Dronning Maud Land, Antarctica). For previously published spatial and chemical data, reader is referred to Riley et al. (2005) and Heinonen et al. (2013).

Sample	Z1812.3	Z1816.1	Z1816.2	Z1813.1	Z1816.3	Z1817.2	Z1803.1	Z1803.5	Z1834.3
Subgroup	high-ε_{Nd}	high-ε_{Nd}	high-ε_{Nd}	high-ε_{Nd}	high-ε_{Nd}	high-ε_{Nd}	low-ε_{Nd}	low-ε_{Nd}	low-ε_{Nd}
TiO_2 (wt. %)[a]	4.12	3.34	3.91	3.65	3.26	3.95	4.06	3.61	4.93
FeO_{tot} (wt. %)[a]	13.07	12.87	13.67	13.81	11.08	13.29	12.96	13.04	12.83
MgO (wt. %)[a]	11.91	14.73	14.83	12.70	21.68	12.27	8.66	11.72	9.77
CaO (wt. %)[a]	10.30	8.99	10.14	10.28	7.70	10.14	10.46	9.90	10.74
$^{87}Sr/^{86}Sr$ (i)[a]	0.703650	0.703570	0.703520	0.704070	0.703930	0.703660	0.705510	0.706150	0.705320
$^{143}Nd/^{144}Nd$ (i)[a]	0.512846	0.512867	0.512858	0.512763	0.512771	0.512769	0.512664	0.512676	0.512678
ε_{Nd} (i)[a]	8.6	9.0	8.9	7.0	7.2	7.1	5.1	5.3	5.3
Re (ppb)	0.84	0.83	0.65	0.84	-	0.62	0.36	0.51	0.73
Os (ppb)	1.36	1.31	1.77	1.31	-	1.05	0.63	0.97	0.20
$^{187}Re/^{188}Os$	2.972	3.078	1.771	3.077	-	2.843	2.759	2.548	18.137
$^{187}Os/^{188}Os$ (m)	0.13329	0.13382	0.13042	0.13342	-	0.13331	0.13545	0.13494	0.18252
$^{187}Os/^{188}Os$ (2σ)	0.00006	0.00006	0.00010	0.00011	-	0.00007	0.00009	0.00007	0.00016
$^{187}Os/^{188}Os$ (i)	0.12436	0.12458	0.12510	0.12418	-	0.12477	0.12717	0.12728	0.12804
$^{238}U/^{204}Pb$	10.4	11.9	8.5	10.5	11.3	12.4	9.9	10.1	10.4
$^{232}Th/^{204}Pb$	29.0	34.7	22.2	31.9	36.0	38.1	34.8	36.0	36.1
$^{206}Pb/^{204}Pb$ (m)[b]	18.613	18.573	18.601	17.914	17.706	18.178	18.029	18.048	17.945
$^{207}Pb/^{204}Pb$ (m)[b]	15.536	15.509	15.523	15.362	15.329	15.411	15.426	15.415	15.383
$^{208}Pb/^{204}Pb$ (m)[b]	38.06	38.03	38.07	37.58	37.30	37.71	37.80	37.77	37.67
$^{206}Pb/^{204}Pb$ (i)	18.319	18.235	18.359	17.612	17.385	17.827	17.748	17.762	17.651
$^{207}Pb/^{204}Pb$ (i)	15.522	15.492	15.511	15.347	15.313	15.394	15.412	15.401	15.368
$^{208}Pb/^{204}Pb$ (i)	37.80	37.72	37.87	37.29	36.98	37.37	37.49	37.45	37.35

[a] data from Riley et al. (2005); [b] uncertainty assigned to external error (2σ): $^{206}Pb/^{204}Pb = 0.005$, $^{207}Pb/^{204}Pb = 0.005$, and $^{208}Pb/^{204}Pb = 0.01$.

Supplementary tables S1-S4

Click here to download Supplementary material for on-line publication only: SupplementaryData.xls